Safety and efficacy evaluation of Biosynthesized Nanoparticles

By

Sahibzada Muhammad Uzair Shah Hashmi

(NUST 201463584MASAB92514F)

Atta-Ur-Rahman School of Applied Biosciences,

National University of Sciences and Technology,

Islamabad, Pakistan.

2016

Safety and efficacy evaluation of Biosynthesized Nanoparticles

A thesis submitted as a final year project in partial fulfillment of the requirement for the degree of Master of Science

In

Industrial Biotechnology

By
Sahibzada Muhammad Uzair Shah Hashmi
(NUST 201463584MASAB92514F)
Supervised by: Dr. Hussnain Ahmed Janjua

Atta-ur-Rahman School of Applied Biosciences,
National University of Sciences and Technology,
Islamabad, Pakistan.
2016.

Dedicated to

Muhammad (S.A.W)

Who indeed is the

Love, Mercy and Compassion to the Worlds

The best of Mankind

The light and the ultimate guidance

Repeller of Affliction and Disease

&

My parents for teaching compassion and patience

My brother for being the back bone and the love of my life

Acknowledgements

All praise to my Glorious Lord, Allah the Almighty, the Creator of this Universe, who has always blessed me with a sense of thankfulness, Humbleness and love. The owner of Crown, the repeller of Affliction and Disease, the Master of Madina, Prophet Muhammad (P.B.U.H). I pray t
that He always keeps me under your supervision.

I am thankful to all people who have contributed in my research, inspired me with their ideas and devotion for country and guided me during my stay at NUST. Especially I owe my gratitude to my esteemed supervisor Dr. Hussnain Ahmed Janjua for continuously showing confidence and trust in me always inspiring me to think different and big. I am grateful to Head of Department Dr. Sadaf Zaidi and Principal Dr. Peter John for accommodating me with lab facilities for my research. I am thankful to Dr.Tehseen Alam without which this research was not possible. I would like extend my sincere thanks to all seniors and juniors especially my research group I call 'CRG'. I would like to extend my gratitude to Zain ul arfeen, Danish Gul, Hafsa Khan, Marriam Khurshid and Hurmat Riaz for best of the company during the last year. Lots of love for Aqib Javed-the pundit, tiger-Asad Abdullah, and my Nigga-Talha khan for being Brothers for life. I would like to extend deepest regards to Tahira khan and Faria khan for bearing up with a person like me. You both are gems. No arslan, I didn't forget you. I am thankful to all your criticism and for the discussions about single thing one could think of.

Special thanks to my parents who made me the person I am today. I can't thank you enough for the sacrifices you both have made. And to my brother Hurair, I am thankful for sharing the chemistry never shared between two individuals for bearing my attitude and facing my anger for

all years and counting. I would do anything to make you happy. You indeed are an apple of my eye. Lots of prayer for your bright future. You are born to rule the world. Be sure to do it.

Table of contents

List of Figures

List of Acronyms

ACRONYM	GENERIC NAME
µg	Micro Gram
AgNP	Silver nanoaprticles
AJ	Aerva javanica
AjNPs	Aerva javanica silver nanoparticles
BC	Bowman's capsule
CD	Collecting ducts
CFU	Colony Forming Unit
CNPs	Strach capped silver nanoparticles
DMSO	Di methyl sulfoxide
ELISA	Enzyme Linked Immunosorbant assay
GSH	Glutathione
H&E	Hematoxylin and Eosin
HAI	Hospital acquired infections
HC	Heliotropium Crispum
HCEC	Human colonic epithelial cell lines.
HcNPs	Heliotropium crispum silver nanoparticles
HS	Horse Serum
IP	Intraperitoneal
LB	Luria Bertani
MDR	Multiple drug resistant
ml	Milliliter
mM	Mili Molar
MRSA	Multiple Drug Resistant Staphylococcus Aureus
MTT	3-(4,5-Dimethylthiazol-2yl)-2,5-Diphenyltetrazolium Bromide
PA	Pseudomonas Aeruginosa
pA	Pseudoagar
PALS	Peri-arteral lymphatic sheath
PBS	Phosphate Buffer Saline
PFS	Paraformaldehyde
PVP	Polyvinyl Pyrroliodine
RBCs	Red blood cells
ROS	Reactive oxygen species
RP	Renal pelivs
rpm	Rate Per Minute
SCF	Sulbactum-Cefoperazone
SEM	Scanning Electron Microscopy
SOD	Super oxide dismutase
SPM	Scanning Probe Microscopy

TNF	Tumor necrosis factor
TSB	Tryptone Soya Broth
TZP	Tazobactum-Pipracillin
UV-Vis	Visible Ultra Violet
VNPs	Violacein capped silver nanoparticles
XRD	X-Ray Diffraction
XRF	X Ray Florescence
ZnNO3	Zinc Nitrate
ZnNPs	Zinc Oxide nanoparticles
ZnO	Zinc oxide
ZP	Zeta potential
ZS	Zeta Sizer

Abstract

Extensive utilization of silver nanoparticles have raised concerns of their effects on biological systems. Silver nanoparticles often showing great antimicrobial potential often cannot pass the safety because of their unknown toxicity profile. Nanoparticles synthesized from biological source have additive advantage over chemical source owing to reduction in cytotoxicity. Various synthesis approaches have been developed for the fabrication of silver nanoparticles used for specific application. In vivo assessment hence plays a key role to unveil their effects and interaction with biological system. Current study is designed to compare already biosynthesized nanoparticles for their efficacy and safety profile and screen out the nanoparticles showing highest efficacy profile. Violacein capped silver nanoparticles (VNPs), Starch capped silver nanoparticles (CNPs), Aerva javanica silver nanoparticles (AjNPs), Heliotropium crispum silver nanoparticles (HcNPs), and zinc oxide nanoparticles (ZnNPs) were used for this study. The radical scavenging potential of these five nanoparticles were analyzed through H_2O_2 radical scavenging assay which showed the concentration dependent scavenging activity of nanoparticles. This was followed by the evaluation of their safety profile by performing MTT assay. Histological analysis of these nanoparticles were done through H&E staining to assess the morphological changes in liver, spleen and kidney of the balb/c mice (n=100). Doses ranging from 3mg/kg to 24 mg/kg were given intraperitoneally on daily basis for 28 days and effects were monitored. VNPs showed highest mortality and morbidity rate along with tissue damage as compared to rest of nanoparticles. The *in vivo* activity of these nanoparticles were studied in balb/c mice (n=40) with an infected partial thickness burn (2^{nd} degree). The burned area was seeded with CFUs of $2x10^8$ of Methicillin resistant *Staphylococcus aureus* and *Pseudomonas aeruginosa*. AjNPs along with HcNPs were

screened to pass these experiments and found out to be more efficacious and safe for their use as antimicrobials and disinfectants.

Chapter 1

1 Introduction

Cytotoxicity of Silver nanoparticles has been reported in many studies affecting viability (Medintz, Uyeda, Goldman, & Mattoussi, 2005) and various mechanisms have been studied which are responsible for their cytotoxic effects. Cytotoxicity mechanisms were also shown by immediate production of Reactive Oxygen species (ROS) by damaging mitochondria, there by producing ROS species causing DNA damage leading to apoptosis (Clarke et al., 2009). Surface protection by Polyethylene glycol reduced the cytotoxicity but cellular modification of PEG to PEG-Amine made them cytotoxic once again. Degree to which Silver nanoparticles are cytotoxic is dependent upon various parameters including morphology (size and shape), surface chemistry, capping materials and concentrations of nanoparticles. (Lovric et al., 2005). Nano-biotechnology has opened a new era for research in biomedical sciences; nanoparticles refers to the smallest functional organization of a molecule in the nano-metric scale (1-100nm). Hence, interaction of these individual molecules at cellular and sub cellular levels may provide high specificity with maximum therapeutic and minimum side effects attainable through targeted and tissue specific interactions when applied in clinical settings (Silva, 2004).

Biologically synthesized nanoparticles are efficient drug nano-crystals with many therapeutic potentials including pronounced bactericidal, anti-biofilm and bacteriostatic effects reported in multiple drug resistant bacterial species. Amongst many metallic nanoparticles, silver nanoparticles are best known for their established anti-bacterial effects such as in wound healing, burn and severe infectious diseases treatment, water sterility and as a potent disinfectant(Behra et al., 2013; Dar, Ingle, & Rai, 2013). It is well known that Multiple Drug Resistant (MDR) bacterial strains are emerging in nosocomial infections which renders present antimicrobial drugs and

sterilizing agents in effective. (Schaberg, Culver, & Gaynes, 1991). However, increase in nosocomial infections is inevitable due to ever-changing hospital populations, current procedures employed in patient care such as use of unsterilized surgical and operative instrument and excessive use of antibiotic drugs (McGowan, 1983). It was also observed that bacterial strains of *Pseudomonas aeruginosa* are one of the most common hospital acquired infection agents isolated from wounds, skin and burn patients with high level of MDR reported (Emori & Gaynes, 1993)**.** Hence, with present antibiotics and antimicrobial drugs rendered ineffective, there is a dire need to come up with effective and efficient antibacterial approaches to prevent hospital acquired MDR bacterial infections.

With the advent of nanotechnology in medicinal field and efficacy of metals and their corresponding oxides including silver and zinc oxide having potent antimicrobial and synergic drug effects, a whole new possibility to develop a range of antimicrobial agents is now opened. These antimicrobial agents can be utilized to prevent the spread of MDR nosocomial bacterial infections through different means such as by topical application of nanoparticle ointments and gels in burn and wounds (L. Huang, Dai, Xuan, Tegos, & Hamblin, 2011) (Jain et al., 2009) synthesis of nanoparticle embedded cotton fabric dressing or nanobandages (Rigo et al., 2013) , as disinfectant sprays and nano-coatings in surgical and medical devices to develop microbial control systems (Jun Sung Kim et al., 2007)

In spite of main developments in the controlling severe burn damage in patients, a high morbidity and mortality rate (Horvath et al., 2007) is noted among them. Burn wound damages the protective layer of the skin which acts a barrier to pathogens and opportunistic microorganisms in which immune system plays a significant role along with infection establishment in patients with thermal injuries (Cheppudira et al., 2013). *Staphylococcus aureus (PA)*, particularly methicillin-resistant

S. aureus (MRSA), is the principal source of septicemia in immunocompromised patients owing to presence of burns. 40% of wound isolates represented MRSA. Among all pathogens, MRSA was isolated from Forty percent of wound samples. MRSA when colonized in burn wound patients, a successful infection of 14-17% was established (Dar et al., 2013).

To improve drug release and penetration and to overcome the unmet physiochemical characteristics of drugs various strategies have been adopted. Nanometric system, especially nanospheres possess great surface to volume ratio and hence greater surface area that increases the desired activity of nanomaterials.(Shim et al., 2004). Studies related to nanoparticles incorporation in the hydrogels and their use as topical treatment for burn wounds studies are in their nascent phases. Especially the extent to which biosynthesid silver nanoparticles are studied for their efficacy evaluation from biological sources is very limited (Y. Zhang et al., 2014)

Current research is focused on comparative analysis of biosynthesid silver nanoparticles for their efficacy and safety evaluation in the burn wound infection models. Current study is designed to evaluate following hypothesis.

- If biologically synthesized nanoparticles are capped with extracts that possess anti-oxidant and radical scavenging properties, then these nanoparticles must have innate anti-oxidant activity.
- If they have established antioxidant properties they must not be toxic to primary cell lines, and must be toxic to cancerous cell lines.
- Since the biosynthesid nanoparticles including nanoparticles from *Aerva javanica, heliotropism crispum,* and nanoparticles from *J. libidium* have established antimicrobial profile so they must be effective for controlling infections *in vivo*.

- Since the tissue damage is dependent on size, shape and charges of nanoparticles, biosynthesid nanoparticles with various parameters must show different responses when injected intraperitoneally.

Main objectives of the study was the comparison of already synthesized silver nanoparticles taking into consideration the various activities including

- Radical scavenging activities to monitor the anti-oxidant properties of nanoparticles and to rate the nanoparticles on the extent of anti-oxidant properties, so they may be used in future studies for drug delivery purpose, besides their use as disinfectants.
- MTT Assay to assess the mitochondrial damage in primary cell lines as well as cancerous cell lines including MCF-7, Huh7 cells, Hela Cells, and Human corneal epithelial cell lines.
- Histological analysis through H&E staining to assess the tissue toxicity, inflammation along with the morbidity and mortality rate on exposure to silver nanoparticles.
- Burn wound infection model in balb/c mice to determine the efficacy of biologically synthesized nanoparticles.
- To identify the most safe and efficacious nanoparticle from pool of 5 nanoparticles apparently exhibiting good antimicrobial profile, and safety *in vitro.*

Chapter 2

2 Review of Literature

2.1 Introduction

Science of nanotechnology has revolutionized the manipulation of matter at nano scale by designing and characterizing of nanomaterials. (Goddard Iii, Brenner, Lyshevski, & Iafrate, 2007) it is a well-established fact that properties of materials changes at nano level. Wings of butterfly is one example of nano design by nature which is due to presence of nanoparticle crystal. These nanomaterials promise to further revolutionize our life. Nanoparticles have been known for their interesting optical, electrical, thermodynamic properties(Arias, Gallardo, Gomez-Lopera, Plaza, & Delgado, 2001). Surface Plasmon resonance is an example of one interesting phenomenon exhibited by metallic nanoparticles, while semiconductor nanoparticles show fluorescent properties due to presence of quantum confinement (M. Liu & Guyot-Sionnest, 2004). Wu et al concludes in his paper that large surface area provides nanomaterial advantage over electrical thermal and conducting properties than macro sized materials.

Nanobiology deals with the applications of nanomaterials in living systems. In this respect nanomaterials are currently being used as biosensors and in bioimaging because of their fluorescent properties, as antitumor and antimicrobial agents because of their cytotoxic effects on tumour cells and microbes, in photothermal therapy because of their surface plasmon resonance in magnetic hyperthermia and magnetic resonance imaging because of their magnetic properties (Salata, 2004) (M. Liu & Guyot-Sionnest, 2004)

2.2 Silver nanoparticles a preferred system for Nanobiotechnology

Elemental silver is known for its antimicrobial activity(Jain et al., 2009) and used in burned surfaces (Thakkar, Mhatre, & Parikh, 2010), medical devices (Emerich & Thanos, 2006), in disinfecting water (Sharma, Yngard, & Lin, 2009) in fabrics and in textile garments (Perelshtein et al., 2008). But elemental silver is prone to deactivation followed by complex formation reducing the silver activity and inertness (Chaloupka, Malam, & Seifalian, 2010). Nanotechnology advancement has provided an alternative for its limitation by the growth of silver at nanoscale, the fabrication of silver nanoparticles(S. Liu et al., 2010). These nanoparticles act via ROS production thereby killing microbes through ROS generation (S. Liu et al., 2010)

2.3 Free Radicals and Reactive Oxygen Species

Molecular entities containing an unpaired electron that is capable of existing independently is a free radical. They can either be formed from the electron loss or electron gain. (Cheeseman & Slater, 1993). Another method known as hemolytic fission is a method when the covalent bond is broken from shared pair of electrons resulting in radical formation. (Kassaee, Mohammadkhani, Akhavan, & Mohammadi, 2011). In biological systems production of free radicals occur either by enzymatic or non-enzymatic reactions. Biologically significant free radicals include derivative of oxygen commonly known as Reactive oxygen species or ROS including Superoxide ($^{\cdot}O_2^-$), Hydrogen peroxide (H_2O_2), Hydroxyl radical ($^{\cdot}OH^-$) (Cheeseman & Slater, 1993).

2.4 Beneficial and Harmful Effects of free Radicals

Cells continuously produce ROS and various additional radicals species as a by-product as they perform many critical function. ROS produced by Phagocytes play important part in destruction of bacterial and fungal species. (Curnutte, 2004). Nitric oxide, another free radical functions as

signal transmitter in brain and cardiac system along with its role as relaxant of endothelial lining to maintain blood pressure (Ignarro, 1990).

It has been established that free radicals have a very important role for proper cell functioning when formed at controlled concentrations but as the balance is disturbed oxidative stress occurs. This oxidative stress can either be exogenous (alcohol, drugs, tobacco smoke, pesticides, and air pollutants) or endogenous (intracellularly through multiple mechanisms including NADPH oxidase Complex. The unpaired electron cause the free radical to immediately react with cellular structures in vicinity attacking to capture their electrons through oxidation resulting in a oxidation cascade leading towards mutation. Oxidative stress has been related with progression of tissue damage, cancer, and in the process of aging.(Konorev, Hogg, & Kalyanaraman, 1998). ROS are not only capable of base pair mutations in DNA (Maynard, Schurman, Harboe, de Souza-Pinto, & Bohr, 2009), but also Lipid peroxidation (Beevi, Narasu, & Gowda, 2010).

2.5 Role of Reaction oxygen species in cancer

Cancer, which is 2nd leading cause of death, is a multifactorial diverse disease (Surh and Na, 2008). Cancerous cells possess significant features including immune evasion, apoptosis escapes, high glycolytic rate, and low radical scavenging activity (Verrax et al., 2009). Oxidative stress plays a vital part in cancer establishment (Kim et al., 2009) by depleting available antioxidants including Superoxide dismutase (captures O^{-2}), Catalase (Captures H_2O_2), Glutathione peroxidase (Captures OH^-) hence increasing the concentration of ROS (Verrax et al., 2009)

On comparison with healthy cells, cancerous cells typically possess elevated amounts of ROS stimulating proliferation and promoting genetic instability. This is primarily because of upregulation and stimulation of oncogenes, and secondarily due to high metabolic rates. This provides an opportunity for cancer biologists to target the redox homeostasis against which

cancerous cells are vulnerable. One of the reason of ROS accumulation is the inhibition of antioxidant defenses by antioxidant enzyme impairment during oncogenesis.(Trachootham et al., 2006).

2.6 ROS dependent Cytotoxicity of Silver Nanoparticles

Chemically synthesized silver nanoparticles have been shown cytotoxic effects because of generation of ROS (Martindale & Holbrook, 2002). Effects of AgNPs have been seen on numerous cell lines including Huh7 cell lines, MCF 7, HepG2, NIH3T3 (Hsin et al., 2008). Precise mechanism depends on size and capping agents of AgNPs but chemically synthesized silver nanoparticles reduced the glutathione (GSH) levels and promotes the production of ROS.(Dewanjee, Maiti, Sahu, Dua, & Mandal, 2011). GSH is an important ROS scavenger, hence play a significant part in minimizing oxidative stress by binding to ROS (Anderson, Nilsson, Eriksson, & Sims, 2004). It's been shown that AgNPs facilitated oxidative stress is because of inhibition of GSH synthesizing enzyme thereby increasing oxidative stress inside cell. However, superoxide dismutase and catalases are also inhibited by silver nanoparticles (Hsin et al., 2008). Cell membrane undergo lipid peroxidation and DNA and mitochondrial damage occurs as a result of ROS generation. Cytochrome C released from mitochondria causes upregulation of Caspase 3 and 9. This release is due to deactivation of Bcl-2 and up regulation of Bax leading to cellular apoptosis which is caused by AgNPs. Biosynthesized nanoparticles, however, do not exhibit cytotoxic properties because of surface capping which potentially reduces their toxicity (Abdel-Aziz, Shaheen, El-Nekeety, & Abdel-Wahhab).

2.7 Antioxidant properties of biosynthesized silver nanoparticles;

Total Phenolic content of a plant determines the mechanism of AgNP synthesis from Plant extract (Abdel-Aziz et al.) Phenols and flavanoids exhibit good antioxidant and reducing properties (Pietta, 2000) that can be employed for AgNPs synthesis (Martínez-Castañón, Niño-Martínez, Martínez-Gutierrez, Martínez-Mendoza, & Ruiz, 2008). As these phenol groups are oxidized quinoid compounds are produced which have the ability to bind to the surface of nanoparticles responsible for capping and stability of nanoparticles (J. Huang et al., 2007) Hence, the synthesized nanoparticle will be capped with antioxidant capping agent thereby reducing the cytotoxicity of these nanoparticles.

2.8 Role of ROS in antibacterial mechanism of Silver nanoparticles

Silver nanoparticles have shown to induce antibacterial effect through ROS production by destroying glycosidic bonds linking Peptidoglycan monomers. (Li, Xu, Chen, & Chen, 2011). This allows bacteria to gain access to plasma membrane and alter its permeability, thereby disturbing the functionality of ATP pumps leading to cell death. This would lead to leakage of cellular content. (Feng et al., 2000). Silver ions released from the core binds to NADH dehydrogenase hencing enhancing the ROS production targeting cellular machinery and disrupt the replication process (Morones et al., 2005). Silver ions released in the presence of AgNPs may interact with some thiol (sulphur containing) groups in enzymes forming Ag-S bonds, which then alters the function of the bacterial enzymes (Feng et al., 2000; Matsumura, Yoshikata, Kunisaki, & Tsuchido, 2003). Also Ag^{+} acting like a weak acid may also intercalates with DNA to form a weak acid-base interaction which then results in bacterial cell damage. Similarly, ZnO nanoparticles interferes with bacterial DNA to switch on genes that can subsequently increase ROS formation inside bacteria cell (Klueh, Wagner, Kelly, Johnson, & Bryers, 2000). Enzyme inhibition induced

by Ag-S bonds also interferes with tans membrane energy generation inside bacterial cells which in turn induces the formation of more ROS (Yamanaka, Hara, & Kudo, 2005).

2.9 Nosocomial infections and pathogens

Antibiotics emerged as the wonder-drugs to combat against bacterial infections in 20th century, however emergence of multiple drug resistant bacterial strains has evoked a new threat to global public health (Levy & Marshall, 2004) . Emergence of multi-drug resistant pathogens are becoming a huge concern for healthcare industry due to increased morbidity and mortality associated with MDR infections. Similarly, health care costs are on increase due to the extra efforts required to control such pathogens (Kittler, Greulich, Diendorf, Koller, & Epple, 2010). *Pseudomonas aeruginosa* is a principal source of nosocomial infections and at present it poses a great threat as a multiple drug resistant pathogen (Aloush, Navon-Venezia, Seigman-Igra, Cabili, & Carmeli, 2006). Similarly, Acinetobacter baumannii has also emerged as a multiple drug resistant pathogen over last few decades, with increased epidemic reported in hospitalized and critically ill patients (Dijkshoorn, Nemec, & Seifert, 2007). Other pathogens such as vancomyicin resistant *Staphylococcus aureus* is also being increasingly isolated from patients with hospital acquired infections and these resistant strains impedes the treatment of infectious diseases worldwide(Tomaszewska et al., 2013).

2.10 Control of Biofilm formation in Nosocomial infections

Anti-biofilm therapy is important to control the spread of chronic infections by biofilm forming pathogen since these persistent microbial infections are not treatable with conventional antibiotics(Costerton et al., 2003). Many pathogens such as *Pseudomonas aeruginosa* has the ability to adhere to surface through alginate extracellular DNA, proteins and exopolysaccharides secretion for biofilm formation(Kalishwaralal, BarathManiKanth, Pandian, Deepak, &

Gurunathan, 2010). The planktonic cells adhere to a surface and proliferate through slow growing colonization of bacterial cells in initial phases of biofilm formation. Bacterial colonies then enter maturation phase through induction of quorum sensing molecules. In the end, biofilm matrix undergoes fragmentation and detachment which causes free dispersion of planktonic cells from biofilm matrix to spread infection (Taraszkiewicz, Fila, Grinholc, & Nakonieczna, 2012). Silver nanoparticles have known bactericidal and anti-biofilm effects which makes them ideal antibiofilm drug candidates. Upto 95% biofilm inhibition has been reported in literature following treatment with silver nanoparticles(Kalishwaralal et al., 2010). Such biofilm inhibition potential makes silver nanoparticles as an ideal coating agent to control catheter coated infections in hospital settings (Danese, 2002). Nanoparticles synthesized from biological source will provide low cytotoxicity profile in conjugation with enhanced therapeutic effect in such a system.

2.11 Role of Hydrogels and dressings as antimicrobials

Hydrogels are currently being researched in conjugation with antimicrobial materials for better wound healing (Bueno, Bentini, Catalani, & Petri, 2013). Hydrogels are three-dimensional structures based on networks of polymers that can retain significant amounts of water. Hydrogels have numerous biomedical uses such as tissue engineering, drug delivery etc. due to their biocompatible, biodegradable and also viscoelastic nature which enables them to mimic the extra cellular matrix. These properties of hydrogels make them excellent for wound dressings as they facilitate cell viability, migration, proliferation and differentiation (Slaughter, Khurshid, Fisher, Khademhosseini, & Peppas, 2009) Chitosan is an organic polymeric compound with a structure similar to that of cellulose, and vast applications (Eijsink, Hoell, & Vaaje-Kolstada, 2010; "-Nanofibrous Structure of Chitosan for Biomedical Applications,").

Nano-silver wound dressing has emerged as a potential microbial control agent over the last few years which has opened up the prospect to control the spread of hospital acquired infection through incisional wounds, burn and skin patients (Rai, Yadav, & Gade, 2009). The effective phenomena through which Ag bound to surgical dressing and exhibit antimicrobial and anti-inflammatory action, is control release of Ag^{+} ions from Ag nanoparticles embedded in dressing matrix (Wilkinson, White, & Chipman, 2011). Several studies have suggested that silver nanobandages exert antimicrobial, anti-inflammatory and fibrogenic modulatory effect on wounds which not only increases healing potential but also enhances cosmetic appearance of the wound (Tian et al., 2007). Several innovative methods have been suggested for preparation of nanoparticle embedded dressing such as silver nanoparticle embedded bacterial cellulose (Maneerung, Tokura, & Rujiravanit, 2008)and silver coated gelatin fiber mats(Rujitanaroj, Pimpha, & Supaphol, 2008).

With the advent of nanotechnology in medicinal field and efficacy of metals and metal oxide such as silver and zinc oxide having potent antimicrobial and synergic drug effects, a whole new possibility to develop a range of antimicrobial agents is now opened. These antimicrobial agents can be utilized to prevent the spread of MDR nosocomial bacterial infections through different means such as by topical application of nanoparticle ointments and gels in burn and wounds (L. Huang et al., 2011; Jain et al., 2009) synthesis of nanoparticle embedded cotton fabric dressing or nanobandages (Arora, Jain, Rajwade, & Paknikar, 2008; Rigo et al., 2013), as disinfectant sprays and nano-coatings in surgical and medical devices to develop microbial control systems(J. S. Kim et al., 2007).

2.12 Delayed wound healing due to infections

Microorganisms that are usually confiscated to skin gets access to underlying tissues upon skin injury. The extent of infection is dependent on the wound type. Invasive infection is because of

replicating organism being replicating in tissues after the burns (Edwards & Harding, 2004). Inflammation being essential to wound healing owing to contamination removal mostly of microorganisms and prolonged inflammation (cytokines IL-1, TNF- α is a sign of incomplete microbial completion. This may lead for wound to chronic state after the healing failure. This upregulates the matrix metalloproteases, to degrade extracellular matrix. That reduces the level of natural protease inhibitors (Menke, Ward, Witten, Bonchev, & Diegelmann, 2007).

Burn Wound infections are also inhabited by bacteria including Methicillin resistant *Staphylococcus aureus* and *Pseudomonas aeruginosa* in the form of biofilms that secrete extracellular polysaccharide matrix making the biofilms resistant to treatment (Davis et al., 2008).

Chapter 3

3 Materials and Methods

3.1 Radical Scavenging assay.

H_2O_2 radical scavenging assay was performed to assess the radical scavenging activity of biosynthesized silver nanoparticles. The assay was carried out with 96-well plates where 5 nanoparticles including Voilocin capped nanoparticles, starch capped nanoparticles, Heliotropium crispum nanoparticles, Aerva javanica and zinc oxide nanoparticles were used in the study in the varying concentrations of 1 ug/ml, 1.5mg/ml as explained in results section.

A 4 mM solution of H2O2 was prepared in phosphate-buffered saline (PBS: pH 7.4) at 20 C. H2O2 concentration was determined spectrophotometrically at 230 nm absorption Nanoparticles were dissolved in DI water then added to the H2O2 solution final concentration of 1500, 1000, 500, 250, 125, 62.5, 31.25, 16, 8, 4, 2, 1, ug/ml at 20°C. Absorbance of H2O2 was determined 10 min later in a spectrophotometer .Mixing ratio of 1:1 was sued in the study.

3.2 Preparation of Horse Serum supplemented RPMI media

RPMI sachet (Gibco) was added in autoclaved distilled water to makeup solution volume up to 900ml. This was followed by addition of 2g sodium bicarbonate. 100 ml of horse serum (Gibco) was then added to make 10 % HS-RPMI media.

3.3 Trypan Blue Exclusion Assay

Trypan blue exclusion assay was used to check the no. of living cells, cell confluency and cell counting was done by taking 20ul of Huh7 cells, Hela cells and Human corneal epithelial cell lines in 1.5ml eppendorf and adding 20 ul of trypan blue in ratio of 1:1, gently mix the trypan blue with cells using micropipette. After 30seconds, 10ul of sample was loaded on to haemocytometer and

covered with cover slide. Haemocytometer was observed under light microscope to count living cells. Only dead cells were stained blue by trypan blue. Cells per ml were calculated using following formula

$$C = C_{Avg} \times D.F \times 10^4$$

where C is the number of cells per ml, C_{Avg} is the average number of living cells, D.F is the dilution factor calculated using following formula

$$D.F = \frac{\text{cell solution volume + trypan blue volume}}{\text{cell solution volume}}$$

3.4 Cell lines Dilutions and Trypsinization

Cells that reached upto 1×10^6 cells/ml were diluted. Supernatant from T25culture flasks (Corning) was removed and PBS was added to remove suspended cells. 1ml of 0.25% trypsin (Gibco) was added to suspend adherent cells by incubating flask for 5 minutes at 37^{o}C in incubator at 5% CO_2.

3.5 Cryopreservation of cell lines

80% confluent cells were trypsinized and incubated for 5 minutes, and diluted by adding fresh media. Media containing cells transferred into 15 ml falcon (Corning), was centrifuged at 500 rpm for 5 minutes at 4^{o}C. Pellet was resuspended in 5ml of 1X PBS after supernatant was discarded and centrifuged at 300 rpm for 5 minutes. Supernatant was replaced by 900 µl of HS supplemented RPMI media.100 µl of Dimethyl Sulfoxide (Sigma Aldrich) was added and cells were resuspended. Resulting solution was transferred into a cryovial (Corning) and stored at -20^{o}C for 48 hours and was then stored at -80^{o}C for 72 hours and to -150^{o}C for prolonged storage.

3.6 MTT assay for assessing cytotoxicity of Fluorescent silver nanoparticles

3-(4,5-Dimethylthiazol-2yl)-2,5-Diphenyltetrazolium Bromide reduction assay was performed on 96 well cell culture plates (Costar) and method was modified from Kim et al 2009. 5mg of MTT was dissolved in 1ml PBS. Effect of Nanoparticles at different concentrations of 5µg/ml, 7.5 µg/ml, 10 µg/ml, 12.5 µg/ml, 15 µg/ml, 17.5 µg/ml, 20 µg/ml, was checked at 5, 10, 15, 20, 24, 36, and 48hours to assess the cytotoxicity of biosynthesized fluorescent Nano silver. 10 µl of MTT was added in each well and was incubated at 37^{o}C for 2-4 hours. MTT solution from each well was removed and 50 µl DMSO was added to each well to dissolve Formazan crystals. After 10-15 minutes, absorbance was measured at 590 nm and 630nm by ELISA Plate reader (BioTek). Absorbance was translated into graphs and percentage viability was calculated using following formula

$$\%\text{viability} = \frac{(S_{Abs} - B_{Abs})}{(U_{Abs} - B_{Abs})} \times 100$$

Where S_{Abs} is the absorbance of sample, B_{Abs} is the absorbance of blank, U_{Abs} is the absorbance of untreated cells.

3.7 Nanosilver Dilution Preparation for MTT

1mg of nanoparticles were suspended in 1 ml of DI water to make a concentration of 1mg/ml. for 5 µg/ml, 5 µl of 1mg/ml was dissolved in 995 µl of DI water. Similarly, for 10 µg/ml, 10 µl of 1mg/ml stock solution of nanosilver was dissolved I 990 µl of DI water. Remaining dilutions were made following the same protocol.

3.8 Safety analysis of Nanoparticles administration in balb c mice.

0.2ml of nanoparticle solutions were administered intraperitoneally each day for up to 21 days. And the mice mortality and morbidity were calculated through physical examination and alteration in the weight.

3.8.1 Tissue processing for histological analysis

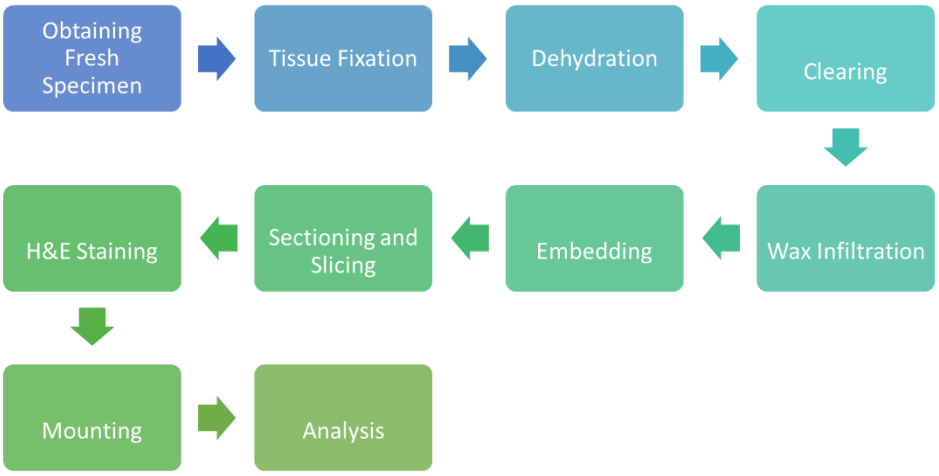

3.8.2 Fixation

Liver, kidney and spleen tissues were isolated after continuous administration for up to 21 days Hematoxylin and eosin staining was performed to histologically analysis the effects of biosynthesid silver nanoparticles in study preserved in 10% formaldehyde solution overnight for processing

3.8.3 Dehydration

A typical dehydration sequence for specimens not more than 4mm thick was used through the microtome (Berleke Biosystems)

70% ethanol 15 min

90% ethanol 15 min

100% ethanol 15 min

100% ethanol 15 min

100% ethanol 30 min

100% ethanol 45 min

At this point all but a tiny residue of tightly bound (molecular) water should have been removed from the specimen.

3.8.4 Clearing

Xylene was used as a clearing agent and to displace ethanol completely. Xylene was used three times with following time

Xylene 20 min

Xylene 20 min

Xylene 45 min

3.8.5 Wax infiltration

Paraffin wax was used to infiltrate tissues at 62^0C to form ribbons for microtome. The process was repeated to remove the xylene and ethanol. Specimens used in the study were not more than 4mm thick. Wax was added three times as following

Wax 30 minutes

Wax 30 minutes

Wax 45 minutes

3.8.6 Embedding

Molds were used to embed tissues in the tissue Cassettes through wax. Prior to embedding tissues were washed used the following solvents.

Solvent	Time
70% Ethanol	1hr
90% Ethanol	1hr
100% Ethanol	1hr
100%xylene	1hr

After washing tissues were fixed in molten wax in the molds and cassettes were place over them. The molds were then placed at -20^{o}C for 20 minutes. Cassettes were the separated for tissue sectioning.

3.8.7 Sectioning

For tissue sectioning, tissues samples were taken out of the paraffin and cut into small layers which are 1-2 cell thick. Microtome sliced the tissues at a thickness of 3-7 um. And the paraffin ribions that were floating on the warm water were placed on the microscopic slides that contained tissues as well. Tissues were then incubated for 30 minutes at 38^{o}C for thorough drying.

3.8.8 H&E staining

Place slides containing paraffin sections in a slide holder (glass or metal)

Slides containing paraffin sections were place in a slide holder. It was followed by deparaffinization and rehydration, followed by hematoxylin staining, eosin staining and dehydration and finally mounting

3.8.8.1 Deparaffinization and sections rehydration

3 x 3´ Xylene

3 x 3´ 100% ethanol

1 x 3´ 95% ethanol

1 x 3´ 80% ethanol

1 x 5´ deionized H2O

3.8.8.2 Hematoxalin staining

1 x 3´ Hematoxalin

Rinse deionized water

1 x 5´ Tap water (to allow stain to develop)

Dip 8-12x (fast) Acid ethanol (to de-stain)

Rinse 2 x 1´ Tap water

Rinse 1 x 2´ Deionized water

3.8.8.3 Eosin staining and dehydration

1 x 30 sec Eosin (up to 45 seconds for an older batch of eosin)

3 x 5´ 95% ethanol

3 x 5´ 100% ethanol (blot excess ethanol before going into xylene)

3 x 15´ Xylene

3.8.8.4 Mounting slides using DPX

Drop of DPX was placed on the slide using a micropipette to avoid entrapment of air bubbles. Coverslip was allowed to gently fall onto slides to allow DPX to spread beneath the coverslip.

3.9 In Vivo efficacy evaluation

3.9.1 Depilation and anesthesia

A total of 48 animals were depilated using electric clipper and hair removal cream. Mice were anesthetized by intraperitoneal injections of ketamine (60mg/kg) and Xylazine (10mg/kg). This was followed by anesthesia of Xylazine and ketamine.

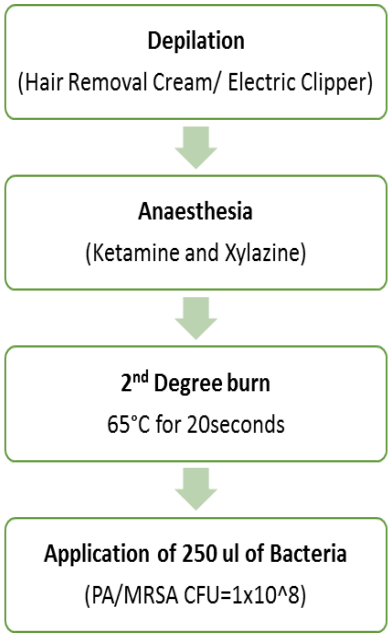

3.9.2 Establishment and conformation of burn wound infection model

Establishment of 2nd degree burn was done by exposing the depilated surface of animals to water at 65^{o}C for 20 seconds. PA and MRSA were used to create infection model. 200ul of PA and MRSA each containing 1x10^{8} CFUs were used to infect balb/c mice. This was confirmed by recovering the bacteria using MRS and pseudo agar.

3.9.3 Topical application of nanoparticles as hydrogels.

Nanoparticles used in the study were incorporated in the chitosan hydrogels. HCNPs and AJNPs were incorporated in the chitosan hydrogels and 2 ml of these hydrogels were applied each day after infection to assess the CFUs reduction.

3.9.4 Formation of Chitosan Hydrogels:

1 g of Chitosan in powder form was weighed using electronic balance and was dissolved in 40 ml 2% Acetic acid with constant stirring by a magnetic stirrer at room temperature for 1 hr. After complete dissolution, 8 ml of 3% Glutaraldehyde solution was added drop wise with constant agitation. Mixture was poured into 10 ml beakers immediately and instant gelation was achieved. The gel formation was checked by the tilt-test 10 ml beakers containing hydrogels to confirm gelation.

3.9.5 Incorporation of Silver Nanoparticles in Hydrogel

Pre-synthesized Silver nanoparticles were added to Chitosan solutions in mixing ratio of 1:3. Afterwards 8 ml of 3% Glutaraldehyde added for gelation. Gel formation was confirmed by the tilt-test.

3.9.6 Determination of bacterial load reduction

Tissue Fluids were collected in 5 ml sterile PBS. This was serially diluted to 10^{-2}, 10^{-3}, 10^{-4}, and plated to calculate CFUs through colony coutner. PA and MRSA was grown on Selection agar which was pseudo agar and MRS agar respectively. Samples collection was done on 1, 3, 7, 11, 15 days. Samples with CFUs with load higher than $2x10^5$ were considered positive for infections.

Chapter 4

4 Results

4.1 Nanoparticles used in the study

Five nanoparticles were used in the study that were synthesised previously. These include Violocin-Capped Silver nanoparticles (V-NPs), Starch capped Silver nanoparticles (C-NPs), *Aerva javanica* Silver nanoparticles (AjNPs), *Heliotropium crispum* silver nanoparticles (HcNPs) and Zinc Oxide nanoparticles (ZnNPs).

Violocin capped silver nanoparticles (V-NPs) are silver nanoparticles with average size of 30nm, and Minimum inhibitory concentration (MIC) of 250ug/ml. C-NPs with an average size of 50 nm have their MIC in the range of 1mg/ml (Sania Arif 2015). AjNPs with average size of 62nm have MIC of 30ug/ml (Hashmi et al 2014). HcNPs with an average size of 40 nm with MIC of 500 ug/ml, ZnNPs with average size of 15nm with MIC of 20mg/ml. (Khan et al 2014).

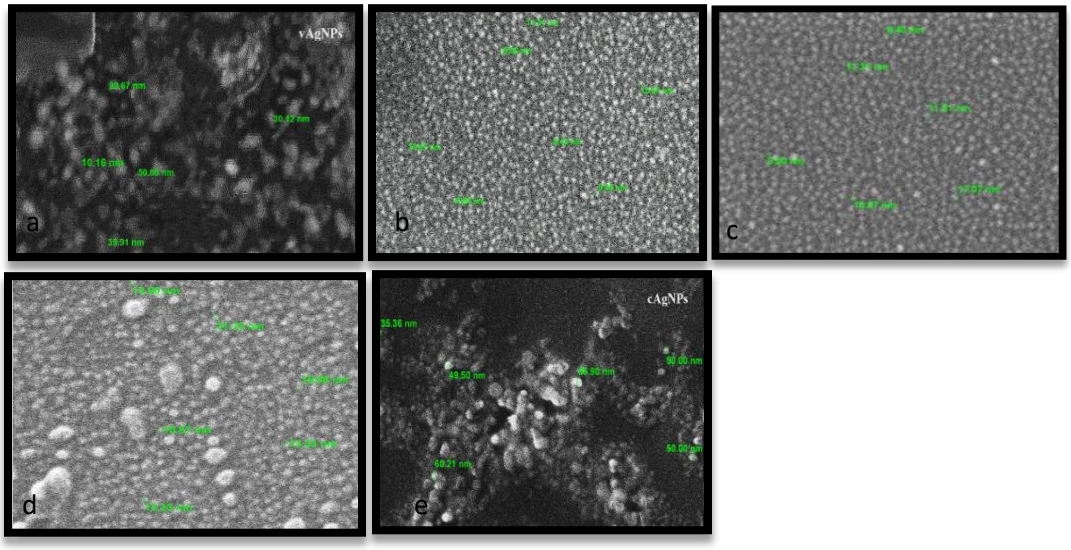

Figure 4.1.1 SEM Analysis of Biosynthesized Silver nanoparticles
A. Violocin capped silver nanoparticles (V-NPs), (B) Aerva javanica nanoparticles AjNPs, (C) Heliotropium crispum nanoparticles (HcNPs) (d) Zinc Oxide nanoparticles (ZnNPs), (e) Starch capped nanoparticles (C-NPs)

4.2 Radical scavenging activity of biosynthesised nanoparticles

H_2O_2 radical scavenging assay was used to evaluate the anti-oxidant ability of 5 biosynthesid nanoparticles. The assay revealed that the scavenging ability of all nanoparticles in the study increases as the concentration of AgNPs increase.

HcNPs showed 5% scavenging at at lowest dose 0f 2.5 ug/ml. The percent scavenging activity was increased proportionally as the concentration increased from 2.5 ug/ml to 2.5 mg/ml. 50% of the inhibition is shown at the concentration of 80 ug/ml. At the highest dose of 2.5mg/ml the percent inhibition of H_2O_2 was upto 75.1 % as shown in figure 2.

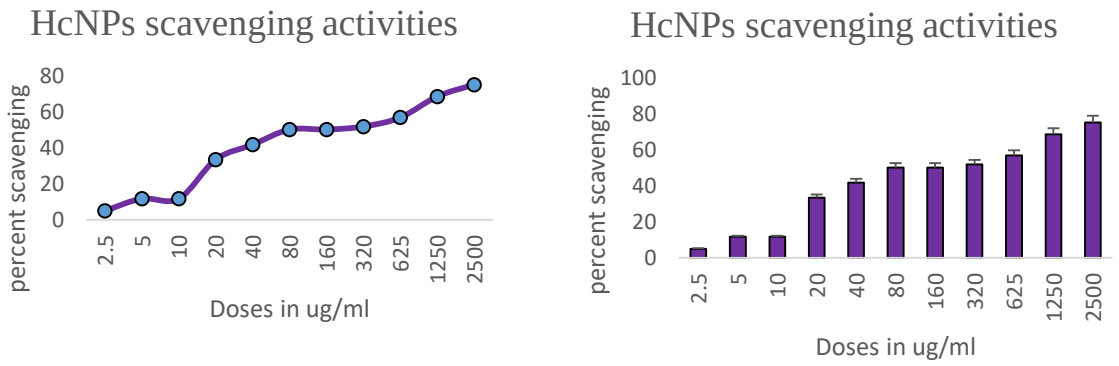

Figure 4.2.1 *% Free Radical scavenging ability of HcNPs at different concentrations*

Similar Trend was shown by AjNPs and its concentration varied from 2.5 ug/ml to 2.5 mg/ml, the percent scavenging increased from 10 % to 76% respectively as evident from the graph. Concentration of 625 ug/ml of AjNPs showed 50 % inhibition of free radicals as shown in the figure 3. This inhibition was increased to 65% at concentrations of 1.25 mg/ml, whereas to 76.1% at 2.5mg/ml.

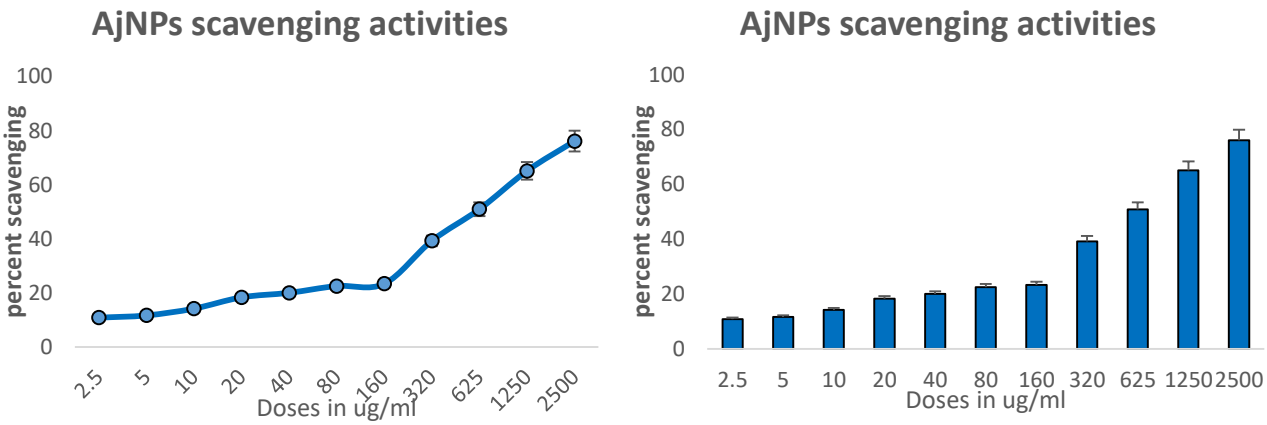

Figure 4.2.2 *Free Radical scavenging ability of AjNPs at different concentrations*

V-NPs showed no activity at the concentrations of 2.5 ug/ml and 5 ug/ml. at the concentrations of 10ug/ml the activity shown was 34% of inhibition. 50 % of the inhibition was shown at the concentration of 80 ug/ml. Maximum inhibition shown by these nanoparticles was 73 % at the concentration of 2.5 mg/ml.

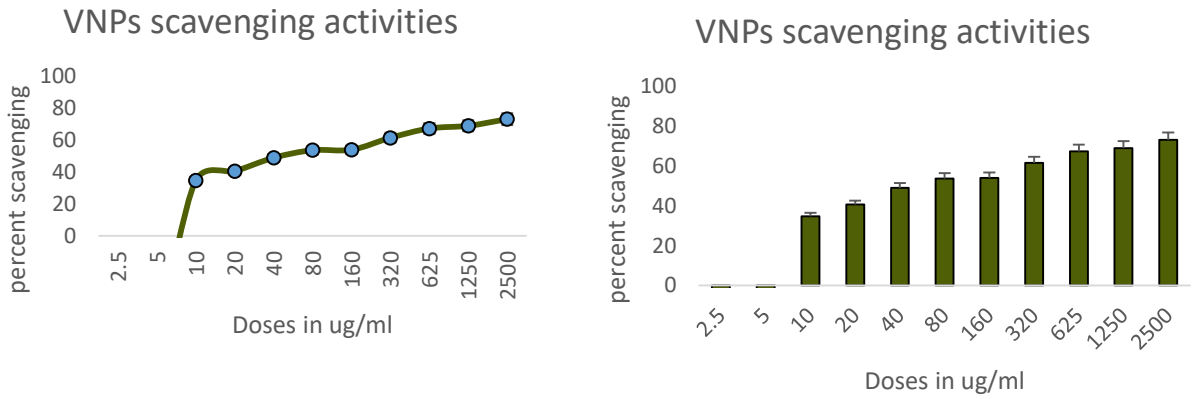

Figure 4.2.3 *Free Radical scavenging ability of VNPs at different concentrations*

C-NPs did not showed scavenging activity at the concentrations of 2.5 ug/ml, 5 ug/ml, 10 ug/ml, 20 ug/ml and 40 ug/ml. at the concentration of 80 ug/ml showed 10% scavenging activity of free

radicals which was just increased to 18% at the highest concentration of 2.5mg/ml.

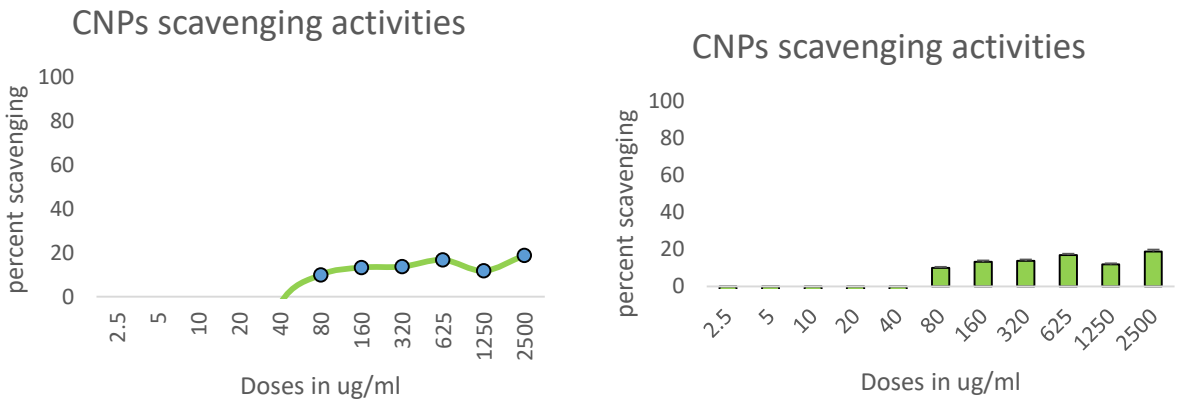

Figure 4.2.4 *Free Radical scavenging ability of CNPs at different concentrations*

ZnNPs on the other hand showed 14% inhibition on the lowest concentration of 2.5 ug/ml, which was increased upto 48.1 % at the highest dosage of 2.5 mg/ml. the increase in the scavenging ability with respect to increase in concentrations was not that much high , as seen in the rest of nanoparticle's activity. Slow increase in the studies were seen as the concentration was increased as shown in the figure below.

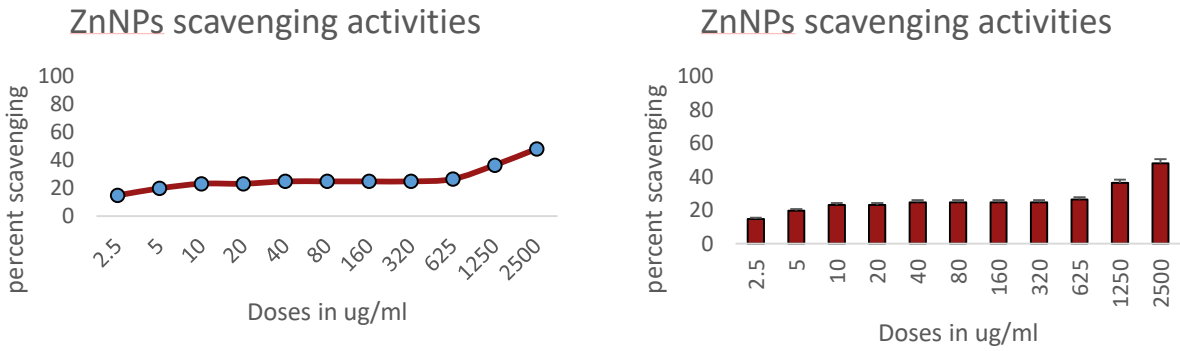

Figure 4.2.5 *Free Radical scavenging ability of ZnNPs at different concentrations*

4.3 Comparison of scavenging activity of biosynthesid nanoparticles.

At the concentration of 10 ug/ml the CNPs shows no activity at all, this was followed by the scavenging ability of HcNPs which was 11%. AjNPs at this particular concentration showed the 14 % of scavenging activity of free radicals. Zinc oxide nanoparticles had greater scavenging of 23 % ability at this particular dosage. Whereas VNPs had greatest scavenging power at the dose of 10 ug/ml of 34 %.

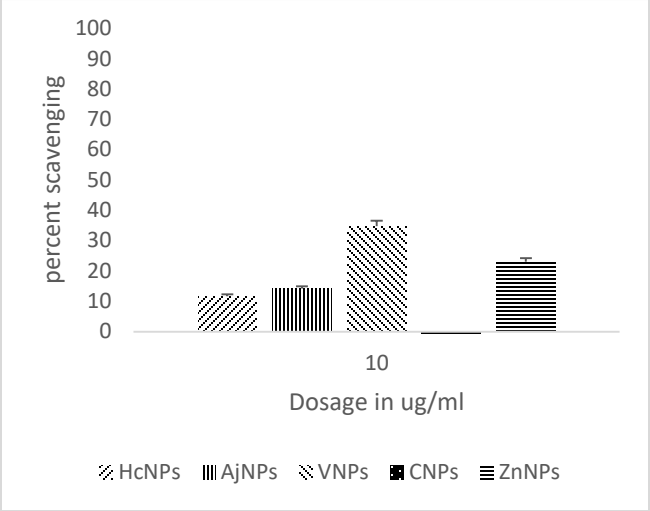

Figure 4.3.1 *comparison of scavenging activities at 10ug/ml*

C-NPs did not show scavenging ability at 20ug/ml but in Scavenging ability of HcNPs were greater (33%) as compared to AjNPs (18%), and ZnNPs (23%). However VNPs still showed higher scavenging power at 20ug/ml as shown in 10 ug/ml.

The scavenging activities of each nanoparticle however was increased as compared to their power at 10ug/l concentration which corresponded to a direct relationship of scavenging power with dose concentration.

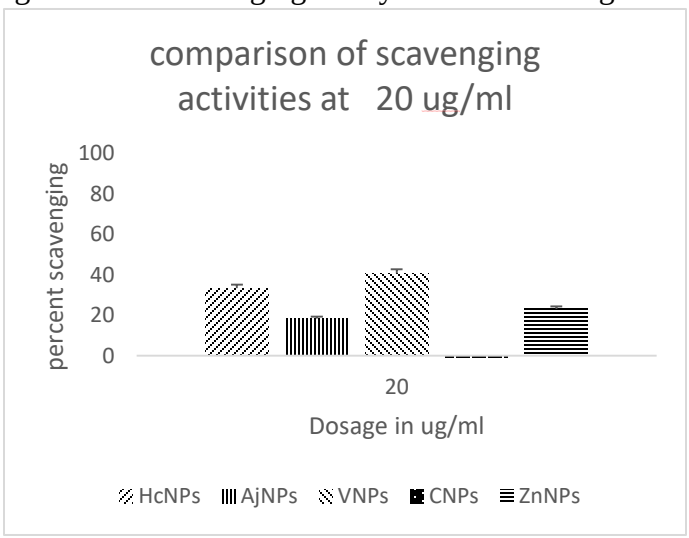

Figure 4.3.2 *comparison of scavenging activities at 20 ug/ml*

At the dose of 40 ug/ml there still was no scavenging ability of CNPs, and the trend observed in at the dose concentration of various nanoparticles continued at the dose of 40 ug/ml as well. The scavenging ability of HcNPs was higher than that of AjNPs and ZnNPs, whereas like previously VNPs showed highest scavenging ability at low dose of 40 ug/ml. HcNPs with % scavenging of 41% at the dose of 40 ug/ml was higher than its power at 20 ug/ml (33%) and 10 ug/ml (10%) . Related trend was witnessed in the case of AjNPs, ZnNPs & V-NPs , that with the increase in the concentration the scavenging power was increased as well.

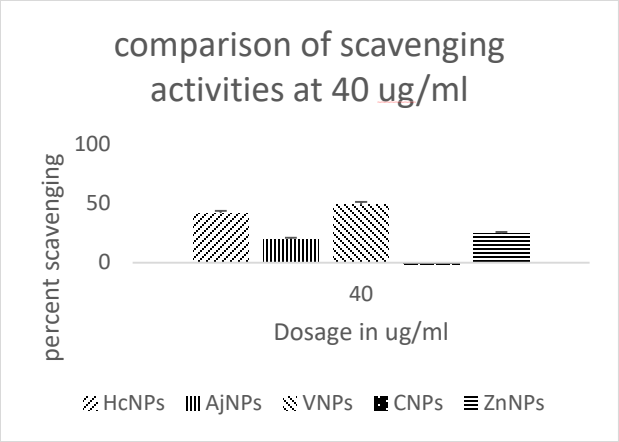

Figure 4.3.3 *comparison of scavenging activities at 40 ug/ml*

Starch nanoparticles (CNPs) at this particular dose showed 10% scavenging at the dose of 80ug/ml. HCNPs showed 50% scavenging activity at this dose and it was much higher than the scavenging ability of AjNPS (22%) and ZnNPs (24%). VNPs at this dose as well showed highest scavenging power of 53 % which was much closer to that of HcNPs (50%) like the trend seen in previous lower doses.

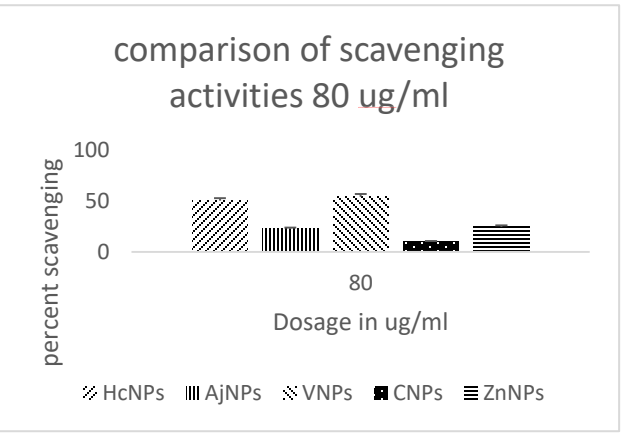

Figure 4.3.4 *comparison of scavenging activities 80 ug/ml*

Increase in the scavenging ability was seen as the dose was increased to 160 ug/ml. this comparison showed the same trend as observed in lower dosage concentration. The scavenging ability of CNPs was increased from 10% to 13 % when the dose was increased from 80 ug/ml to 160 ug/ml. this was lowest increase in the scavenging ability when compared with others. Highest scavenging ability at this dose was found to be of VNPs followed by HcNPs, ZnNPs, AjNPs and lastly CNPs.

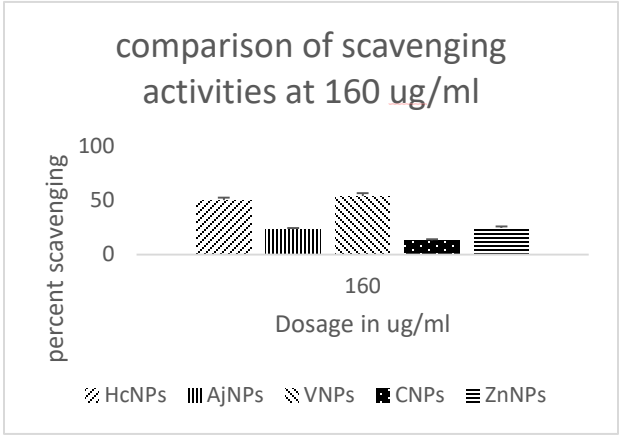

Figure 4.3.5 *comparison of scavenging activities at 160 ug/ml*

The percent increase in scavenging ability when dose was increased from 160ug/ml to 320 ug/ml was much less as compared to the increase when the dose was increased from 80 ug/ml to 160 ug/ml. VNPs still showed highest scavenging power of 61 % as compared to scavenging power of HcNPs (51.8%), AjNPs (39.2%), ZnNPs (24.7%) and CNPs (13.7%). Here the scavenging of AjNPs was higher than the ability of ZnNPs to scavenge free radicals.

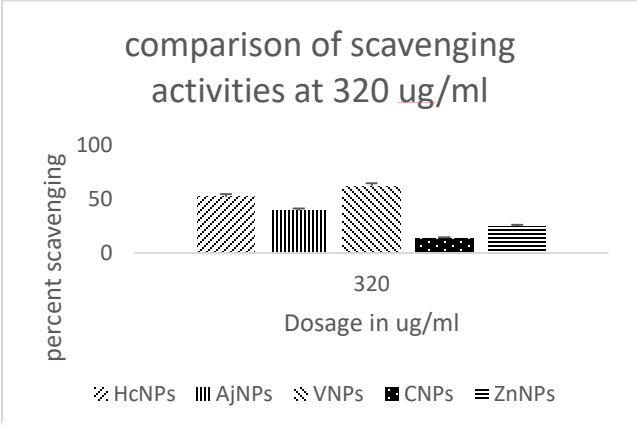

Figure 4.3.6 *comparison of scavenging activities at 320 ug/ml*

AjNPs at this dose showed 50% inhibition of free radicals. But HcNPs (56%) and VNPs (67%) still showed higher scavenging power than AjNPs, CNPs (16.8%) and ZnNPs (26.4%). The ability to

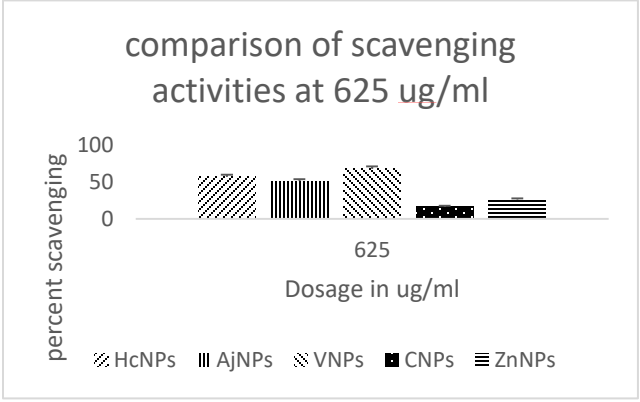

Figure 4.3.7 *comparison of scavenging activities at 625 ug/ml*

scavenge free radicals was seen to be increased as shown by the graphs at independent doses till 10 ug/ml.

AjNPs showed a greater increase in the scavenging power as the concentration was increased from 625 ug/ml (50%) to 1.25 mg/ml (65%). However HcNPs and VNPs were stilling showing higher scavenging percentage of free radical species of 68.5% and 69.08% respectively. CNPs showed decrease in the scavenging power from 16 % to 11% at this concentration which was deviant from the general trend. ZnNPs on the other hand showed rapid increase in percentage from 26.4% to 36.4% at this dose but this 36.4 was still much lower than the percentage of VNPs (69%).

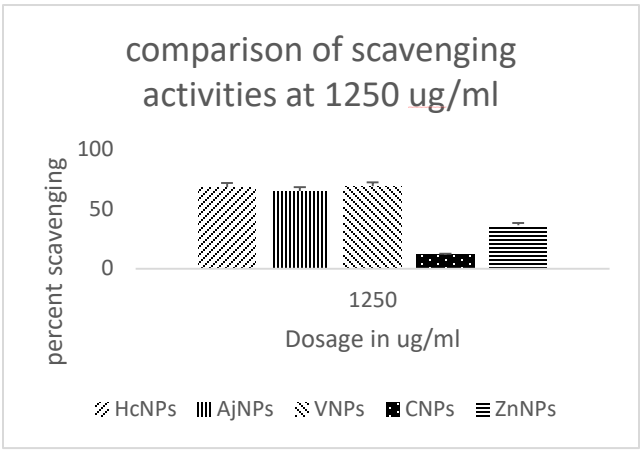

Figure 4.3.8 *comparison of scavenging activities at 1250 ug/ml*

Change in the trend at the highest dose was observed as the AjNPs showed highest scavenging ability of 76.1% from 65%. This was slightly higher than the scavenging ability of HcNPs which was 75%. HcNPs showed high scavenging ability than that of VNPs which was 73%. The scavenging ability of zinc was found out to be 48.13% which was much higher than that of CNPs (18.8%) but lower than radical scavenging power of AjNPs which in this case was 76.1%.

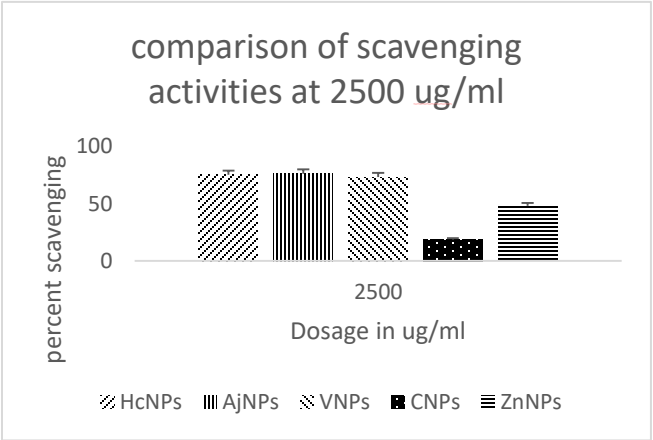

Figure 4.3.9 *comparison of scavenging activities at 2500 ug/ml*

The scavenging power of nanoparticles at lower concentration was dominated by VNPs, but at the highest concentration, AjNPs showed highest scavenging power than the scavenging power of VNPs and HcNPs. The overall trend however showed that VNPs, HcNPs and AjNPs showed similar scavenging activities at

the doses were increased. At low doses VNPs lead the scavenging ability, which was overtook by HcNPs at higher dose and ultimately AjNPs showed high power at highest concentration. Overall VNPs and HcNPs had a slight edge over AjNPs when compared at all doses. This was followed by the Zinc oxide nanoparticles showing maximum scavenging power of 48%. cNPs however showed lowest ability to scavenge free radicals as evident from the radical scavenging assay. The graph below explains the comparison of all nanoparticles used in the study at the concentration ranging from 2.5ug/ml t 2.5mg/ml.

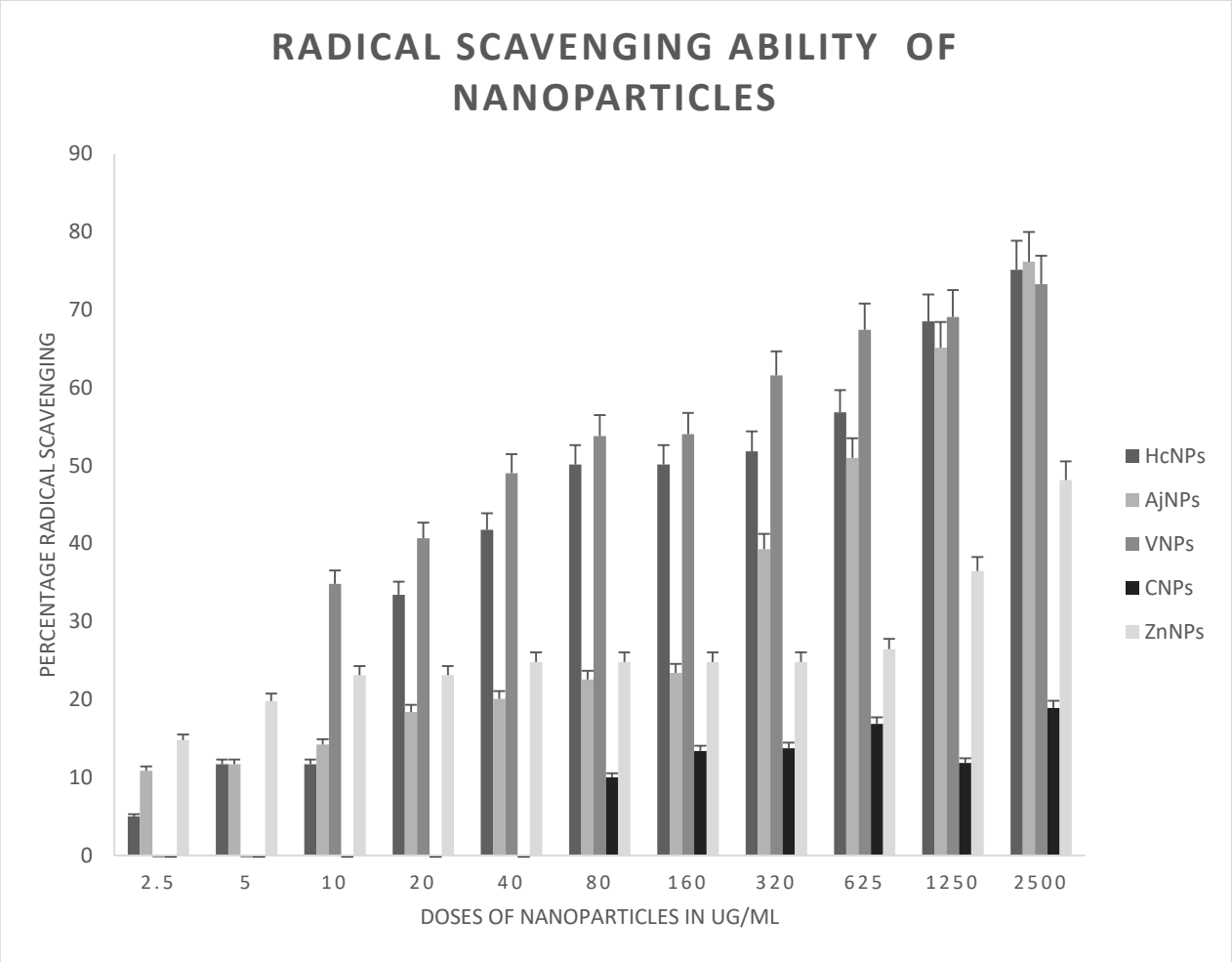

Figure 4.3.10 *Free radical scavenging activities of Biosynthesized nanoparticles on varying concentrations*

4.4 In Vitro cytotoxicity of AjNPs

Cellular cytotoxicity of AjNPs was evaluated on both cancerous cell lines and primary cell lines For cancerous cell lines MCF-7 (breast cancer), Huh7 (Hepatocellular carcinoma) and Hela Cell lines (Cervical cancer) were used and human colonic epithelial cell line (HCEC) was used as a primary cell line to evaluate the cytotoxicity by MTT assay. Behaviour of biosynthesized silver nanoparticles was determined in-vitro.MTT assay was performed to assess the effects of biosynthesized Silver nanoparticles.

Varying concentration of AjNPs were used in this study to assess the effect on various cell lines. On primary cell line HCEC there no reduction in the viability at all concentrations which corresponded to safety of the biogenic silver nanoparticles on HCEC cells. The absence of toxicity in primary cell lines is an indicator of its use as drug delivery vehicle.

This was followed by the assessment of the cytotoxic potential of biosynthesized nanoparticles on cancerous cell lines. Three cell lines mentioned above were used to assess the damage. On MCF-7 cells there no reduction in the viability as compared to the control on varying concentrations of 5ug/ml, to 20 ug/ml. AjNPs were not found to to toxic to MCF-7 cell lines. These results shows they do not possess innate anti-cancer activity for breast cancer cells. Similar trend was observed in the case of Huh-7 cells. Reduction in the activity was not observed at all the concentrations when compared to positive control showing their inability to be use as a drug of treatment for hepatocellular carcinoma (HCC). This however does not exclude its application to be used as drug delivery vehicle in both breast cancer and HCC.

Since AgNPs were compared in this study with other cell lines both primary and cancerous it was evident from the results that AjNPs were safe to use when came in contact with normal cells and

were efficacious against cervical cancer cells while did not kill breast cancer and liver cancer cells and were not toxic to them.

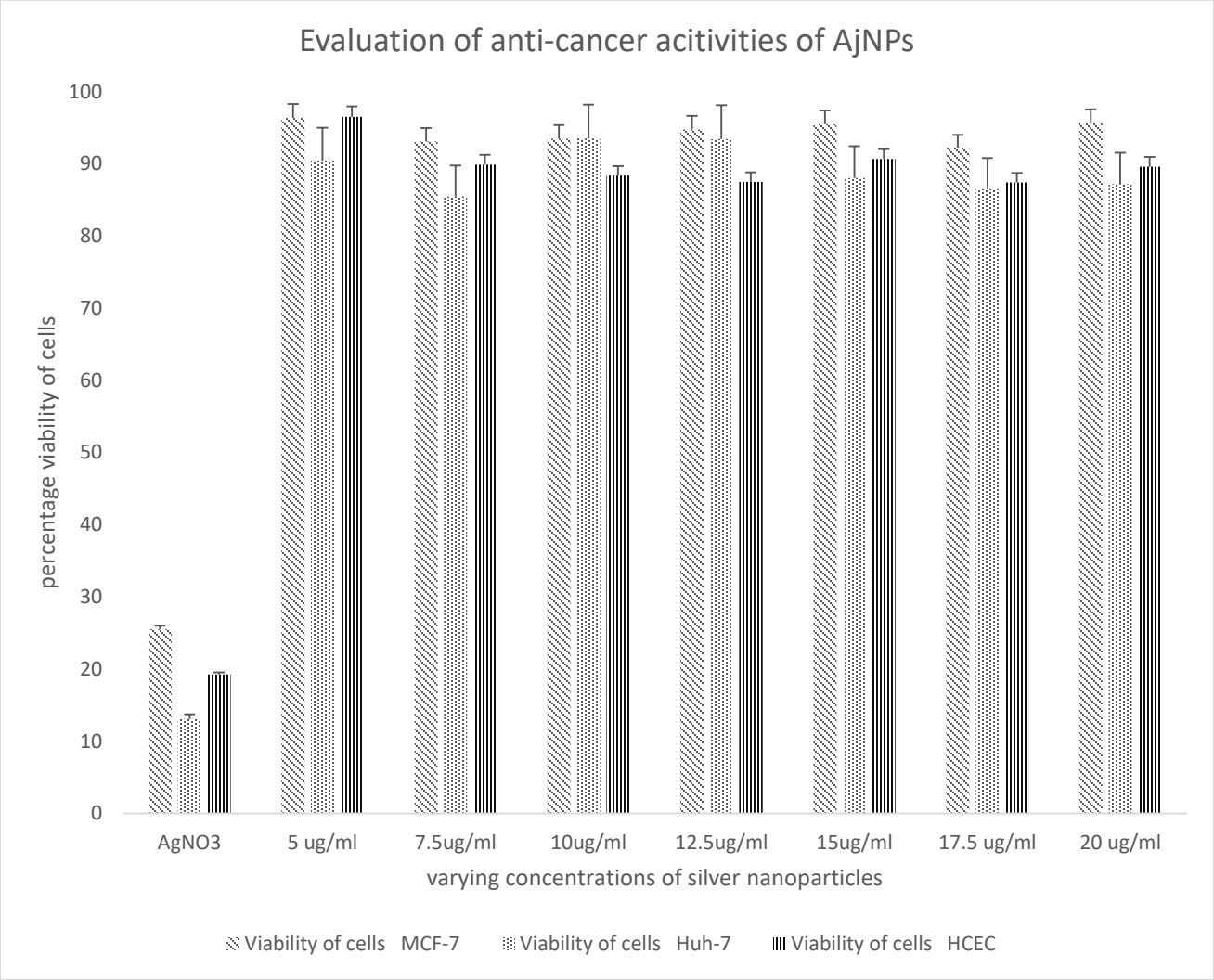

Figure 4.4.1 *Cytotoxicity evaluation of AjNPs on primary and cancerous cell lines*

4.5 In Vivo toxicity assessment of biosynthesized silver nanoparticles: Morbidity Assessment

Spleen inflammation was assessed in balb/c mice by daily injection all nanoparticles with varying dose of 24mg/kg-2.4mg/kg of the mice intraperitoneally for 21 days. HcNPs and AjNPs did not show any signs of spleen inflammation on comparison to rest of nanoparticles. Violocin capped silver nanoparticles showed 12.5 % occurrence in balb/c mice after 21 days f continuous administration. The percentage occurrence of splenomegaly was increased 18.75 % when mice were injected ZnNPs intraperitoneally. Splenomegaly was observed in 25 % of cases when mcie were administered Conjugates of HcNPs and ZnNPs.

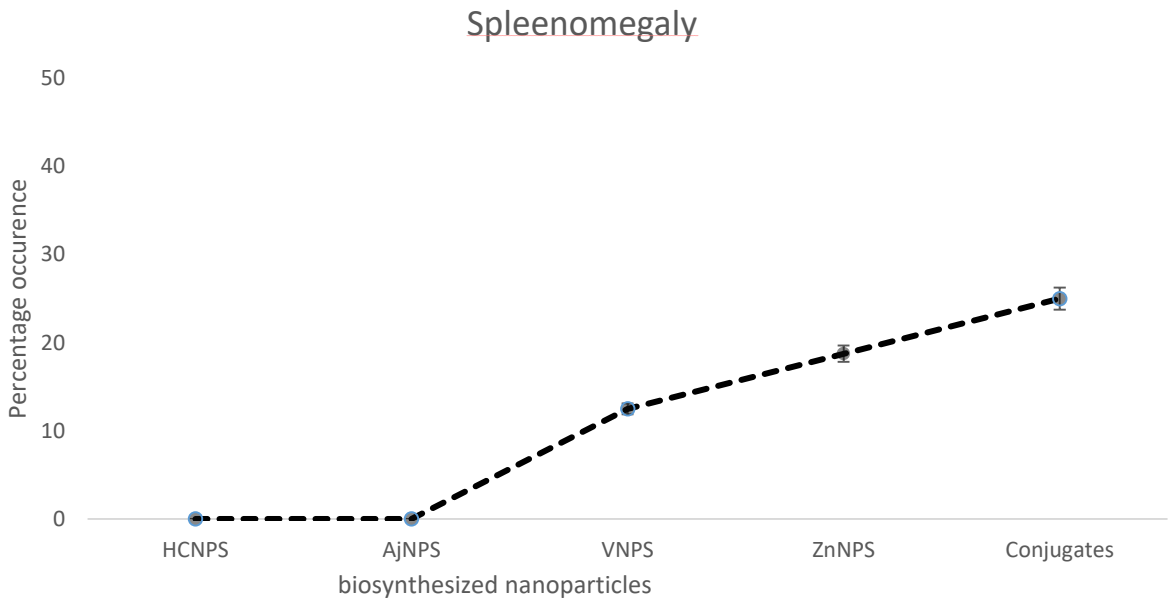

Figure 4.5.1 *percentage occurrence of spleen enlargement in balb/c mice on 21 days administration of various nanoparticles.*

Liver enlargement (hepatomegaly) was also observed in mice after 21 days of nanoparticle administration. Silver nanoparticles synthesized from *Aerva javanica* showed no signs of liver enlargement at all. But HcNPs showed a minute percentage occurrence of 6.25 % when HcNPs were administrated IP. Violocin capped nanoparticles showed greatest percentage occurrence of 25% than other nanoparticles. The percentage occurrence of hepatomegaly when ZnNPs were administered was 12.5% which was increased to 18.75% when they were conjugated with the HcNPs. Here Violocin capped nanoparticles showed high incidence rate of hepatomegaly than rest of nanoparticles and AjNPs did not showed both spleen and liver enlargement. HcNPs on the other hand showed a little incidences of hepatomegaly, while they did not exhibit spleen enlargement in single object. ZnNPs, Conjugates, and VNPs however exhibited both Splenomegaly and hepatomegaly.

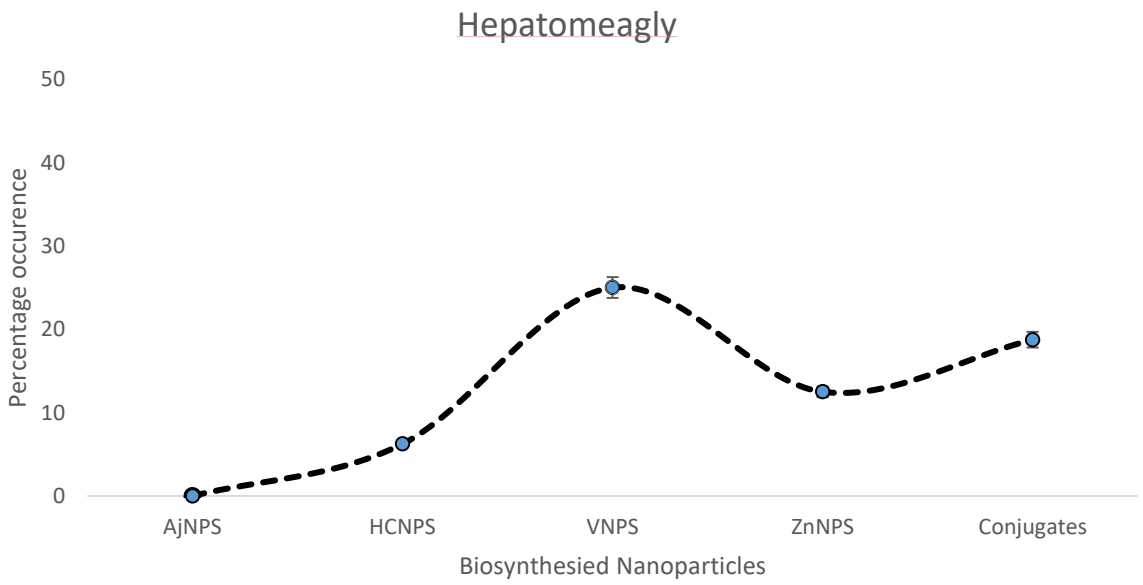

Figure 4.5.2 *Percentage occurrence of Liver enlargement in balb/c mice on 21 days administration of various nanoparticles.*

4.6 Mortality rate assessment

Mortality rate was calculated over 4 weeks and graph was plotted by number of deaths per week against biosynthesid nanoparticles. Violocin capped nanoparticles showed maximum number of deaths with 7 deaths in total which was followed by ZnNPs and Conjugates both exhibited 5 deaths in the span of 4 weeks of administration. Number of death caused by AjNPs were 4 in total with 2 mice died in first week of administration and 1 died in both 3rd and 4th week of administration. Overall VNPs showed highest mortality rate, which was followed by both ZnNPs and Conjugates. Rate of mortality by AjNPs followed death rate from ZnNPs & Conjugates, which was followed by .death rate by HcNPs as explained in the figure below.

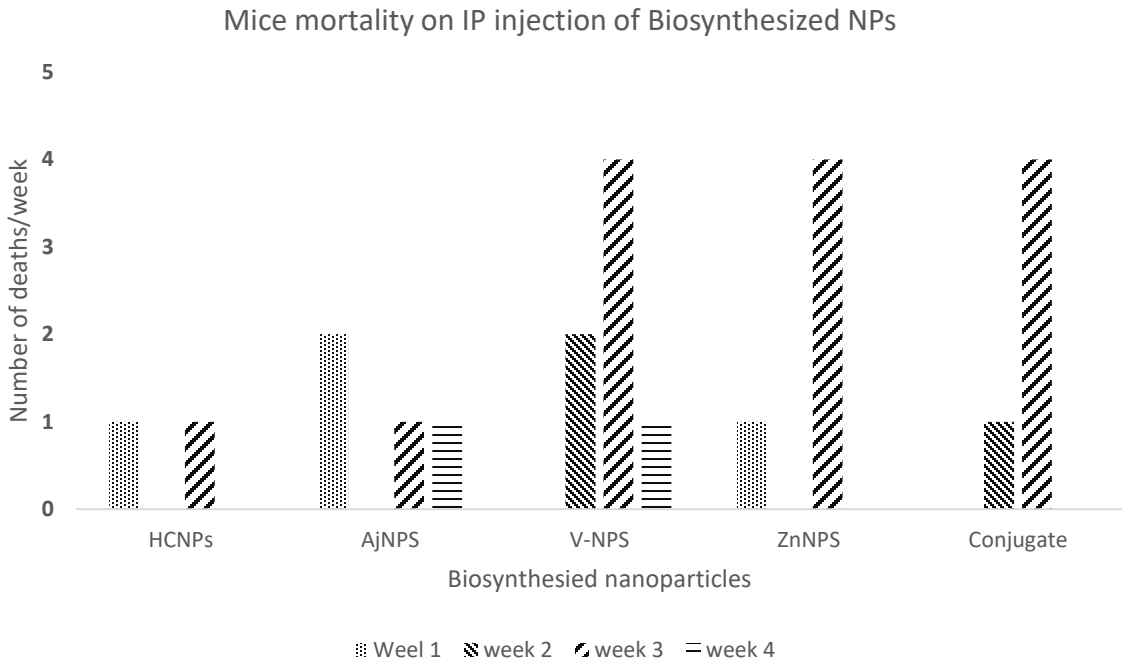

Figure 4.6.1 *Mortality rate on IP injection of Nanoparticles for 4 weeks*

4.7 Weight loss studies

Effect of weight reduction on exposure to biosynthesized nanoparticles was studied over the span of 4 weeks. For HcNPs the weight reduction for dose of 24mg/kg was 42g (first week) to 36 g (4th week). For dose of 12 mg/kg, the weight which was initially 45.4g was reduced to 33.9 g in the fourth week with a small increase in weight during the third week as evident from the figure below. At the dose of 6mg/kg, the weight was reduced from 46g to 37g with a small increase in weight during week 3 of study. For the lowest dose of HcNPs the weight reduction was smallest with average initial weight of 42.9g to 38 g in the final week of study. The small reduction in the weight at low dose corresponded to a linear relationship of drug concentration on weight loss studies for HcNPs as shown in the Figure.

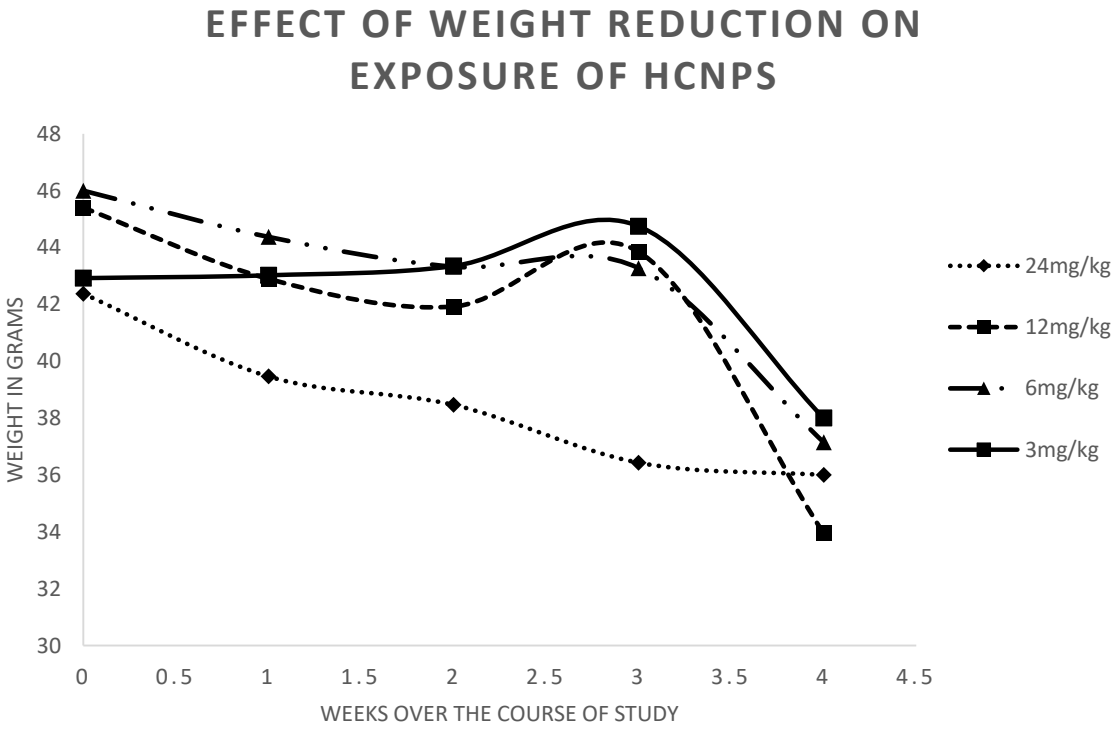

Figure 4.7.1 Effect of weight reduction on exposure of HcNPs

Effect of weight reduction on exposure to biosynthesized nanoparticles was studied over the span of 4 weeks. For AjNPs the weight reduction for dose of 24mg/kg was not seen as at this dose weight was maintained from initial weight of 37.2 g to weight after 4th week of 37.7 g. For dose of 12 mg/kg, the weight which was initially 38.7g was reduced to 37.4g in the fourth week with a small increase in weight during the third week as evident from the figure below. At the dose of 6mg/kg, the weight was reduced from 39g to 33g. For the lowest dose of HcNPs the weight reduction was highest with average initial weight of 42.5g to 36.5 g in the final week of study. The higher reduction in the weight at low dose corresponded that low doses are more significant in weight reduction when compared with the effect of weight reduction at high concentration making an indirect relationship of dose and weight reduction for AjNPs as shown in figure below.

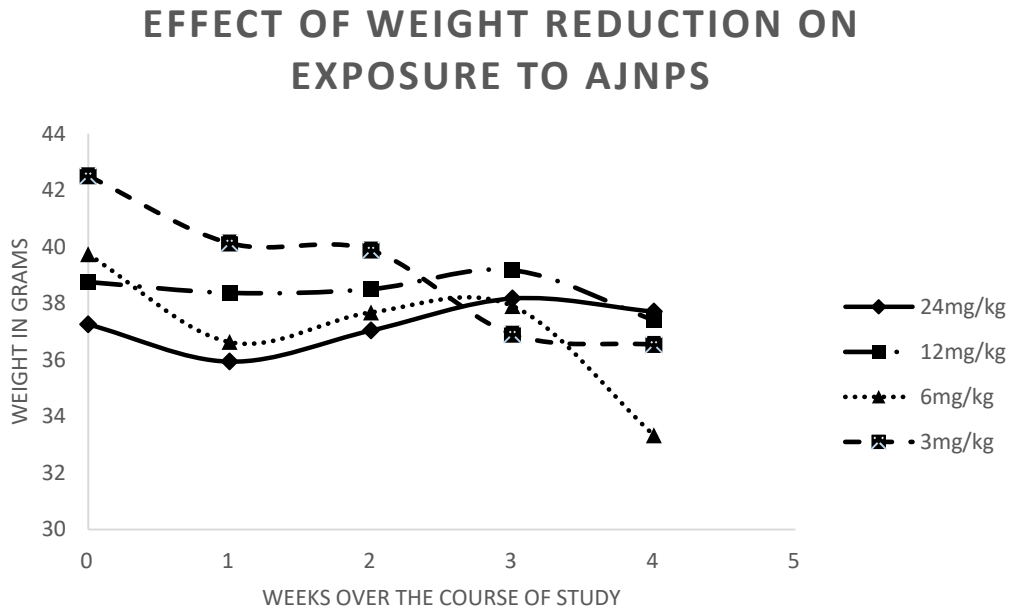

Figure 4.7.2 *Effect of weight reduction on exposure to varying doses of AjNPs*

Effect of weight reduction on exposure to biosynthesized nanoparticles was studied over the span of 4 weeks. For VNPs the initial weight of 40.5g for dose of 24mg/kg was reduced to 34.1g after it was seen at 4th week of study. For dose of 12 mg/kg, the weight which was initially 50.5g was reduced to 36.95 g in the fourth week with a small increase in weight during the third week as evident from the figure below. At the dose of 6mg/kg, the weight was reduced from 44.5g to 39.8g. For the lowest dose of VNPs the weight reduction was highest with average initial weight of 45g to 34.45 g in the final week of study.

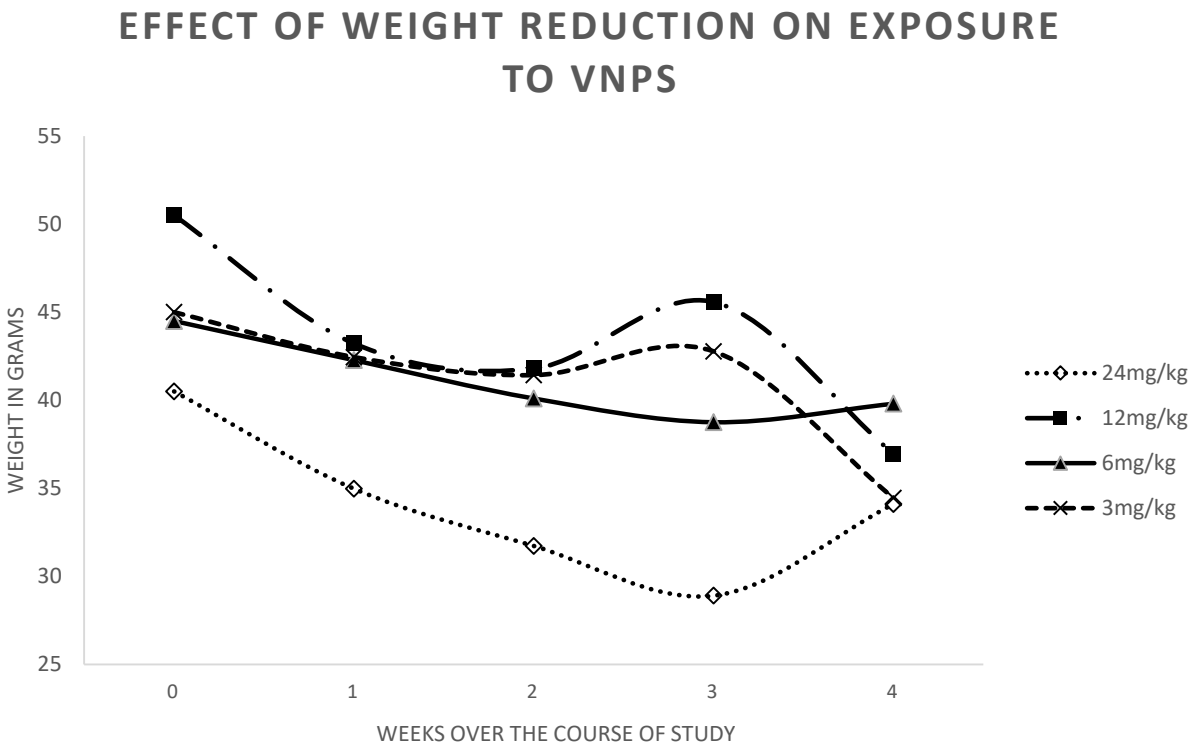

Figure 4.7.3 *Effect of weight reduction on exposure to VNPs*

Effect of weight reduction on exposure to biosynthesized nanoparticles was studied over the span of 4 weeks. For ZnNPs the initial weight of 41.275g for dose of 24mg/kg was reduced to 28.825g after it was seen at 4th week of study. Week 3 showed a small increase in weight as evident from the graph. For dose of 12 mg/kg, the weight which was initially 43.5g was reduced to 34 g in the fourth week with a small increase in weight during the third week as evident from the figure below. At the dose of 6mg/kg, the weight was reduced from 42.125g to 34.35g. For the lowest dose of ZnNPs the weight reduction was minimal with average initial weight of 39.85g to 39.5g g in the final week of study. This corresponded to the direct relationship of nanoparticle dosage with weight reduction as shown in the figure below

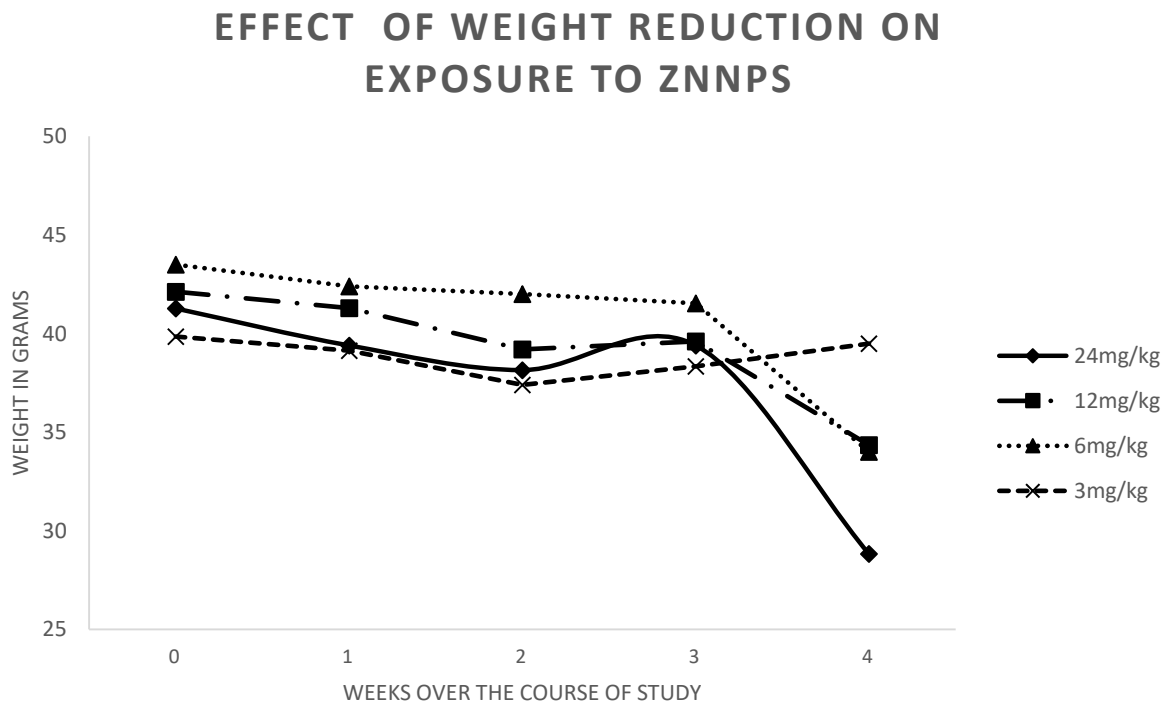

Figure 4.7.4 *Effect of weight reduction on exposure to ZnNPs*

Effect of weight reduction on exposure to biosynthesized nanoparticles was studied over the span of 4 weeks. For Conjugates the weight reduction after 4 weeks was maintained after initial reduction. During the first week the weight was reduced from 38g to 31 g. this was followed by the recovery of weight till 4th week of study to 38.1g.

For dose of 12 mg/kg, the weight which was initially 43.7g was reduced to 37.56 g in the fourth week. At the dose of 6mg/kg, the weight reduction was deviant with initial increase in the weight from week 1 to week 3 which was reduced at week 4. Initial weight of 39.325g was reduced to 30.1g at the 4th week of study. 39.5g g in the final week of study. At the lowest dose of 3mg/kg reduction in weight was seen to be minimal with weight reduced from 43.3g to 36.7g in the last week of study as evident from the figure below.

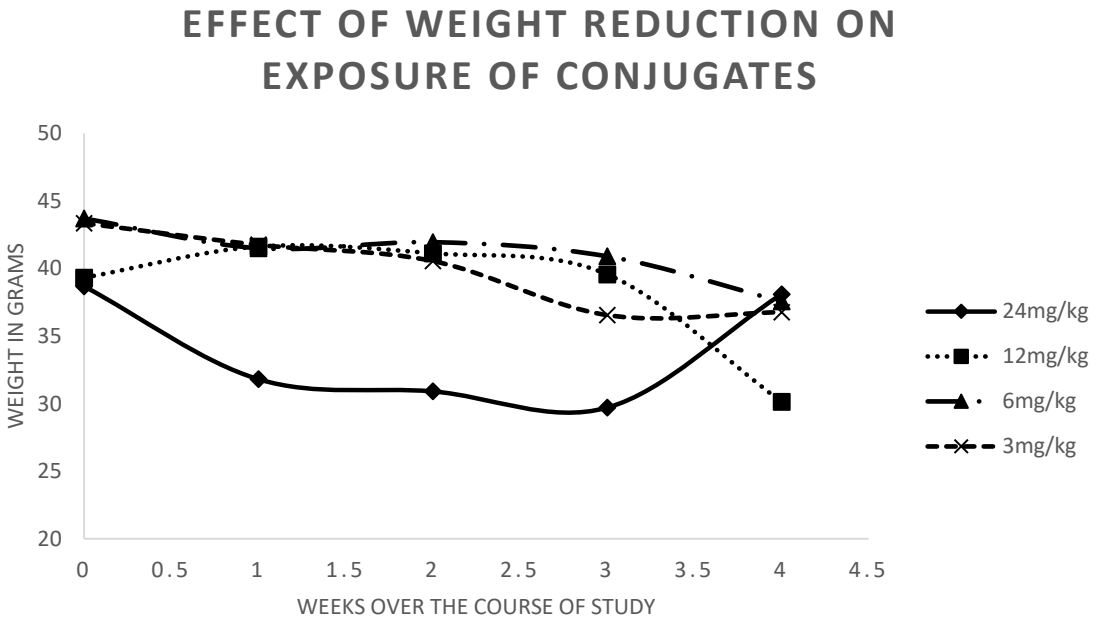

Figure 4.7.5 *Effect of weight reduction on exposure of conjugates*

4.8 Comparative analysis of weight reduction at different doses.

The figure below explains the comparative analysis of 5 nanoparticles used in the toxicity assessment and their comparative weight reduction studies at the dose of 24mg/kg was shown in the figure below. This graph explain the maximum reduction in the weight at this dose was observed in VNPs followed by ZnNPs, conjugates, HcNPs and AjNPs

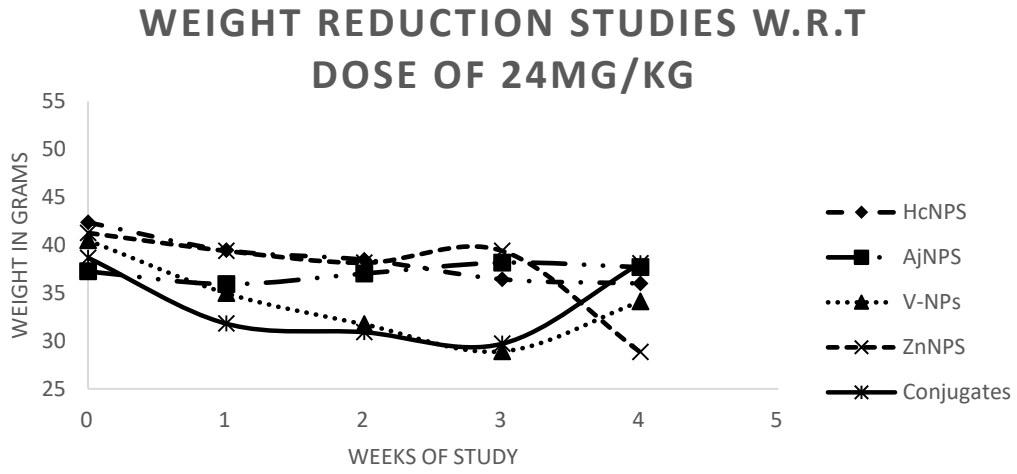

Figure 4.8.1 *weight reduction at dose of 24mg/kg*

(V-NPS > ZnNPs > Conjugates >HcNPs > AjNPs)

Comparative analysis of 5 nanoparticles used in the toxicity assessment and their comparative weight reduction studies at the dose of 24mg/kg was shown in the figure below. At the dose of 12mg/kg vNPs showed greater reduction in the weight while least was shown by conjugates This graph explain the maximum reduction in the weight at this dose was observed in VNPs followed by ZnNPs, HcNPs, AjNPs and conjugates

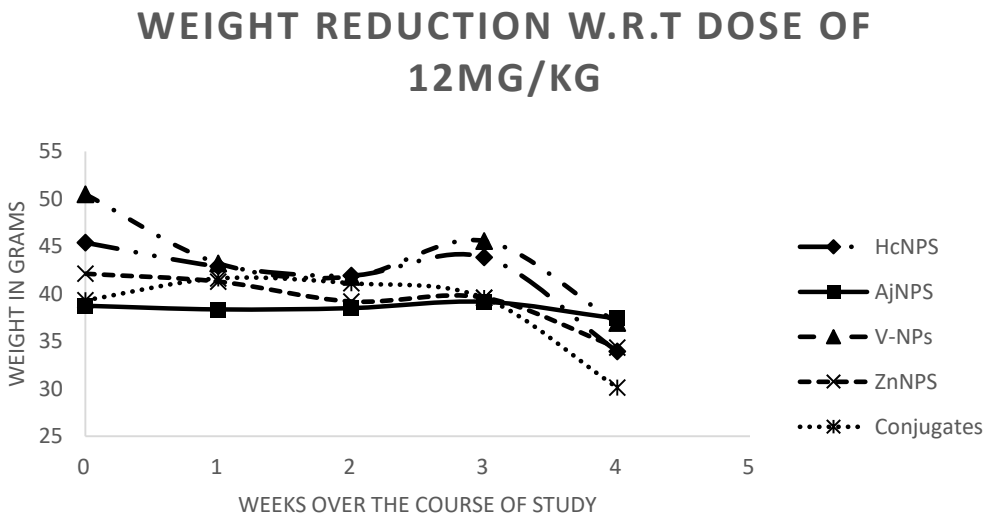

Figure 4.8.2 *weight reduction w.r.t dose of 12mg/kg*

(V-NPs>ZnNPs>HcNPs>AjNPs>Conjugates)

At the dose of 6mg/kg most weight reduction was observed in VNps and least was observed in AjNPs. There was a small increase in the weight during the third week of study which showed the recovery. But that recovery was overcome by the nanoparticles effects as evident from reduction in the fourth week of study. The graph below explains the weight reduction in VNPs followed by conjugates, then ZnNPs and HcNPs and lastly AjNPs

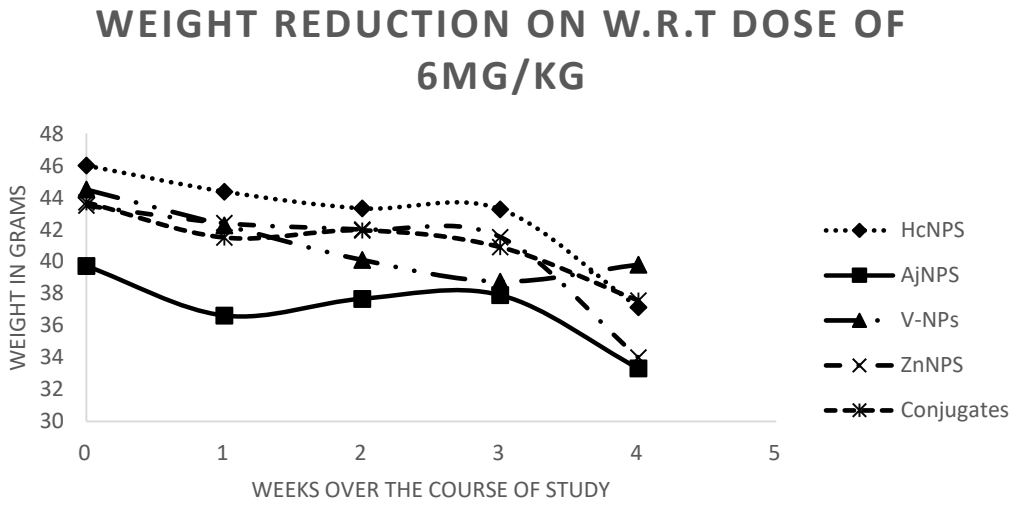

Figure 4.8.3 *Weight Reduction on w.r.t dose of 6mg/kg*

(V-NPs> Conjugates>ZnNPS>HcNPS>AjNPS)

At the dose of 3mg/kg most weight reduction was observed in VNps like in the rest of doses and least was observed in this case in ZnNPs. There was a small increase in the weight during the third week of study which showed the recovery. But that recovery was overcome by the nanoparticles effects as evident from reduction in the fourth week of study. The graph below explains the weight reduction in VNPs followed by conjugates, then AjNPs and HcNPs and lastly ZnNPs

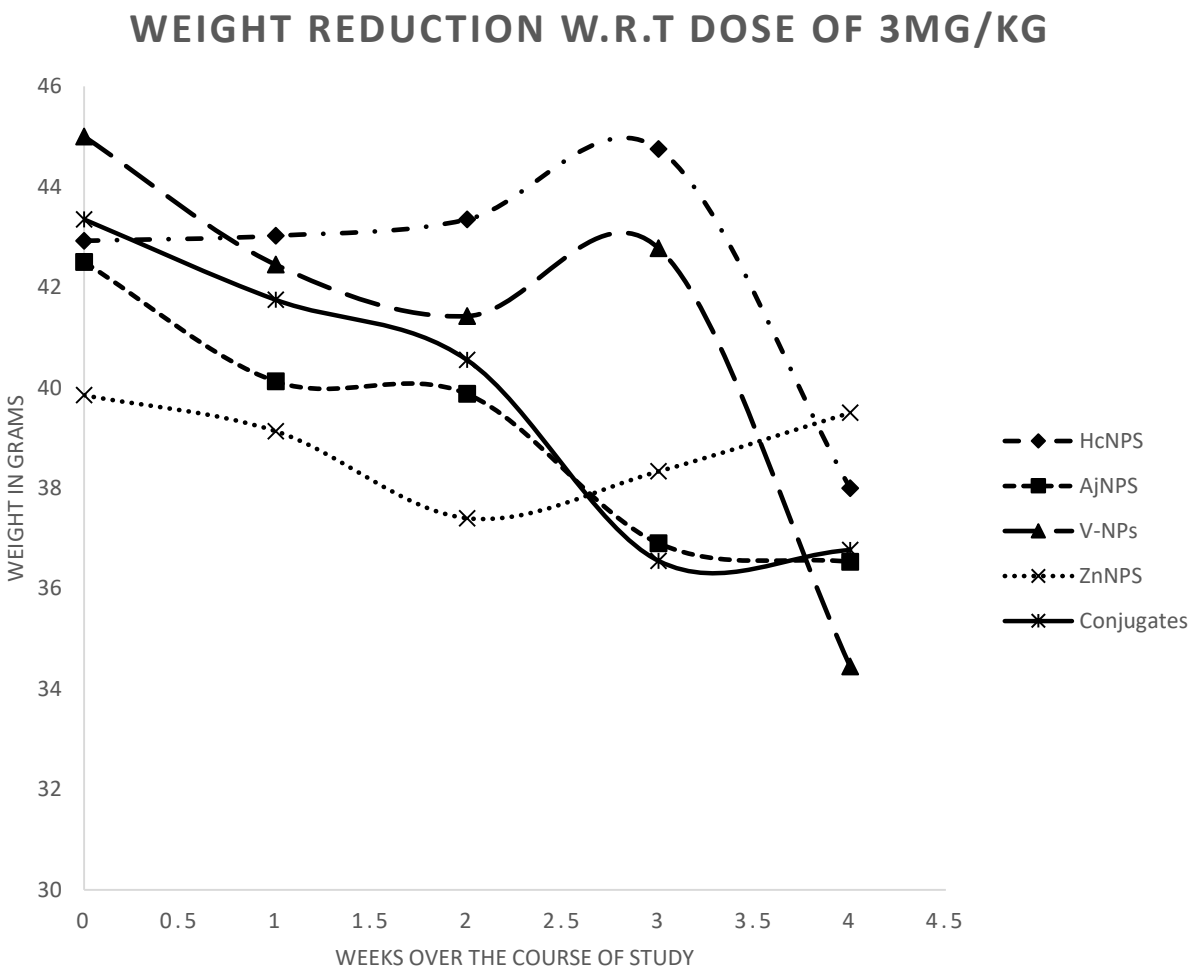

Figure 4.8.4 *weight reduction w.r.t dose of 3mg/kg*

(V-NPs>Conjugates>AjNPs>HcNPS>ZnNPs)

4.9 Histological analysis of Liver, Spleen and Kidney on nanoparticle exposure

Haematoxylin and eosin staining was performed to assess the tissue damage. Liver, spleen and kidney tissues were taken on the basis of the probability that nanoparticle concentration will be higher in such areas owing to the particle size, shape and charge.

4.9.1 Liver Histology

The figure below explains the liver tissues with morphological features of central vein evident in control (a) a larger portal vein can also be seen in the figure which contains bile canaliculi in its proximity. With normal sinusoids along with the hepatocytes with perfectly spherical nuclei as shown in control. HcNPs shows a minute changes in the structure of sinusoids. The hepatic portal vein is evident from the figure (b) along which connective tissue is present. Hepatic triad is visible in this figure and is intact containing the Bile canaliculi adjacent to portal vein is also visible which is responsible to carrying bile synthesised by hepatocytes here in figure. Hepatic artery is shown towards the right bottom of the triad responsible for carrying oxygen and nutrients supplied through sinusoids. Tissue obtained from mice treated with AjNPs has normal histology with small disruption in the sinusoids. Central vein is intact as shown in figure (c), along with the central portal artery and the portal vein's morphology is slightly rough. In case of tissues from VNPs the portal vein can be seen disrupted at some places with intact bile and hepatic artery in the hepatic triad as shown in figure (d). Kupffer cells, which are the macrophages of liver, appear black and dense in colour probably because of VNPs entrapment inside them. ZnNP treated liver tissue upon histological analysis revealed perfect central vein (figure e) which can be differentiated from portal vein owing to absence of connective tissues and absence of portal artery and bile canaliculi in its vicinity. Sinusoids are seen to be leaving the central vein at the bottom of figure however hepatocyte degeneration is shown is evident from the figure. Conjugate treated mice showed a

great extent of liver damage as shown in figure (f) where inflammation of hepatocytes can be seen at the proximal area of figure above the region of central vein. Kupffer cells are shown to be inflamed in these regions showing the nanoparticle intake by liver macrophages.

For liver histology VNP treated tissues showed destruction of both hepatocytes and portal vein with abnormal sinusoids as compared to control and rest of the tissues exhibiting the liver damage on exposure to VNPs along with the engulfment of Kupffer cells which was seen to be enlarged. The inflammation of hepatocytes was also seen in some areas of liver tissue treated with Conjugates.

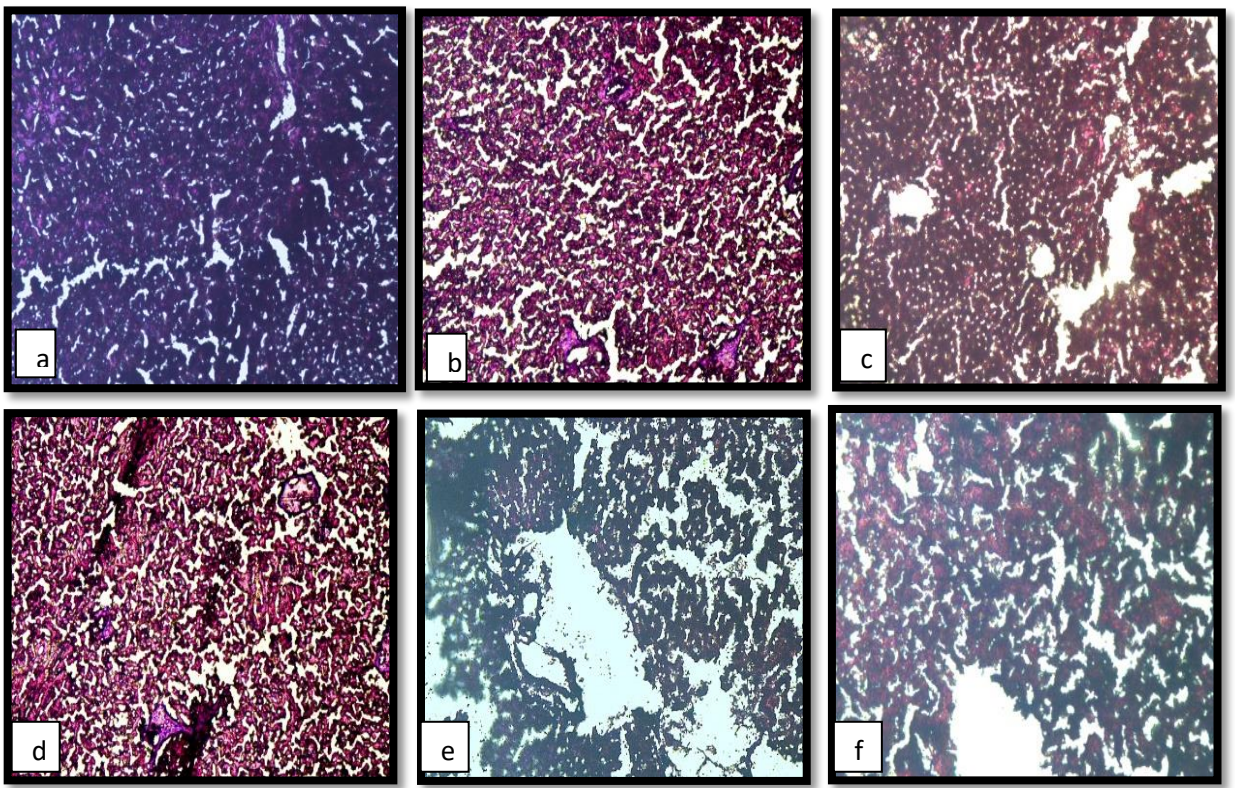

Figure 4.9.1 Histological analysis of liver tissues on exposure to Various Nanoparticles
a) control, (b) HcNPs (c) AjNPs, (d) VNPs (e)ZnNPs (f) Conjugate

4.9.2 Spleen Histology

Spleen is an organ functions in blood filtration destruction of aged erythrocytes, pitting of reticulocytes. It is the site of production of lymphocytes and the antibodies differentiated from plasma cells and activated lymphocytes. Spleen histology was performed to assess the damage caused by biosynthesid nanoparticles on this organ.

Spleen is divided into two segments named red pulp and white pulp as shown in the control (figure a). Usually both red and white pulp share the same percentage in the kidney. Red pulp as showing in the control contains venous sinuses, which are the capillaries extended from the central artery shown in the proximal area of the figure. The area seen as white contains the follicle, marginal zone and the Peri-arteral lymphatic sheath is the white pulp. The dark spots seen in the control are the macrophages which in the spleen are known as histiocytes scans RBCs and removes damaged RBCs from the cells. The smaller circular white dots are the penicillary arteries that are smaller than central arties and are located in the marginal zone.

Figure b represents the tissue section from mice treated with HcNPs. It can be seen that the white pulp in this case covers slightly greater area than red pulp indicating small inflammation. Macrophages appear as large back entity indicating the nanoparticle engulfment in this case owing to the size of HcNPs. AjNPs being smaller in size did not entrap in the macrophages and are not gathered in spleen owing to their small size of 6-8nm. There is an equal distribution of white pulp and red pulp as shown in the figure c. at the bottom of the figure a penicillary artery can also be seen here. Few areas in figure c, however, do show the aggregation of histiocytes corresponding to the possible agglomeration of AjNPs at few points in spleen. Effects of Violocin capped silver nanoparticles on mice spleen is evident from figure d. White pulp which contains follicles

(produces B Cells), Marignal zone (Antigen presenting cells), and Peri-arteral lymphatic sheath (PALS containing T cells)covers around 70% , indicating inflammation in the white pulp area. Abundance of inflamed macrophages are seen at the periphery and reticular fibers are seen as a network indicating the degeneration of red pulp area. ZnNPs shows increase in the amount of nanoparticle captured histiocytes. The bright pink pigment seen in the red pulp area is the hemosiderin can be seen to function in phagocytosis of RBCs being present in the macrophages. The same pigment is present in figure e which is conjugate treated tissue over 28 days and shows the inflammation of red pulp with very little white pulp being shown. Penicillary artery can be seen here along with the inflamed macrophages containing abundant amount of protein hemosiderin secreted usually to break down damaged red blood cells from histiocytes.

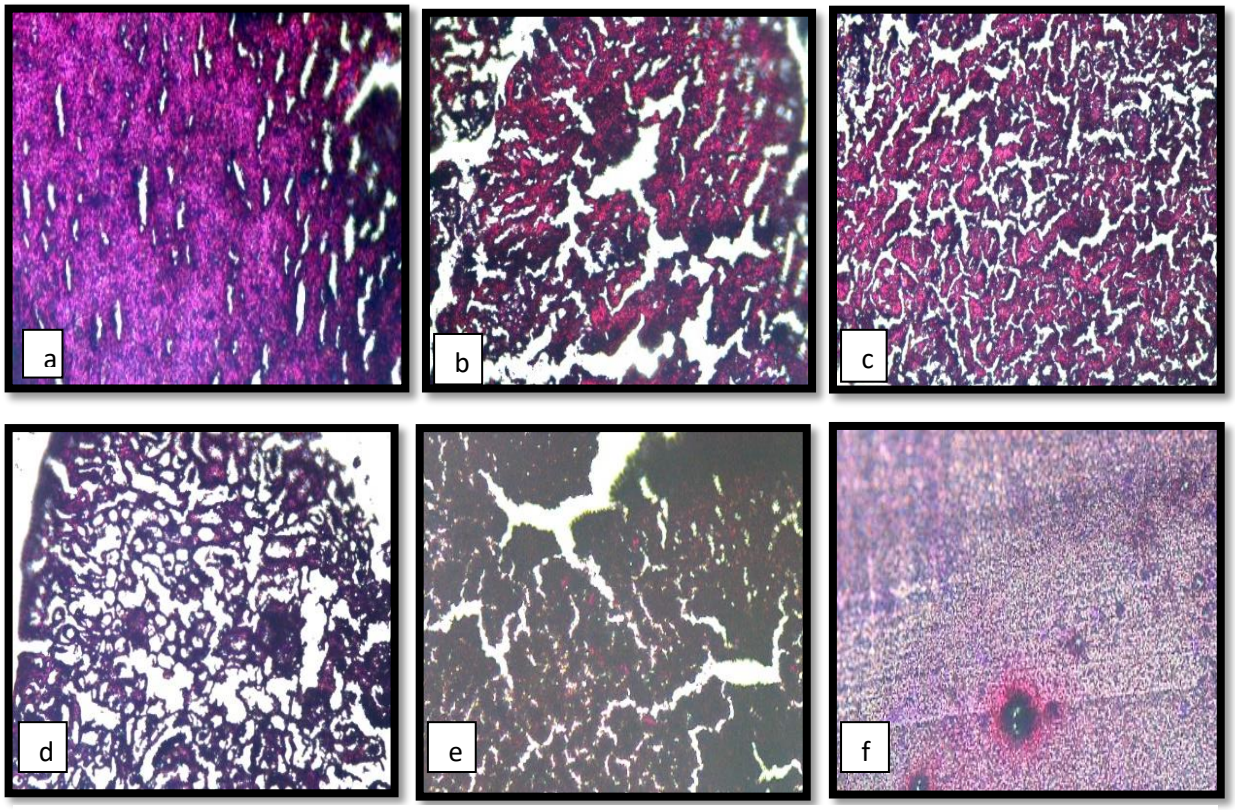

Figure 4.9.2 Histological analysis of Spleen tissues on exposure to Various Nanoparticles
a) control, (b) HcNPs (c) AjNPs, (d) VNPs (e)ZnNPs (f) Conjugate

4.9.3 Kidney histology

H&E staining was done to assess the damage caused by nanoparticles administration and to see the possible entrapment of nanoparticles owing to their physiochemical properties.

Control in Figure a shows the section of renal medulla. And several distilled convoluted tubules are seen here along with interlobular artery. Figure b representing two distilled convoluted tubules. Along with the renal corpuscles containing Bowman's capsule. Figure c represents the tissue slide from the mice treated with AjNPs. These shows the renal medullar portion which is the part of renal pyramid. This magnified portion contains the glomerular filtrate that would dip into the renal papilla that would form minor calyx, which will fuse together to form major calyx that would open into renal pelvis and ultimately into ureter. Figure d represents a minor calyx where the collecting ducts emptied the glomerular filtrate to its way towards ureter through renal pelvis. Figure e represents the transverse section of tissue treated with ZnNPs where medullary rays can be seen along with the collecting tubules with normal morphology. Figure f represents the Conjugate treatment of ZnNPs with HcNPs and its effect on the kidney. This figure focuses on a portion of Bowman's capsule inflamed at from left curve, along with several distilled tubules in the sections. Collecting ducts continuing from distilled tubule can be seen at the left corner of the figure to empty the glomerular filtrate into calyx. No major abnormality is seen except for the partial inflammation of Bowman's capsule when compared to control and standard slides.

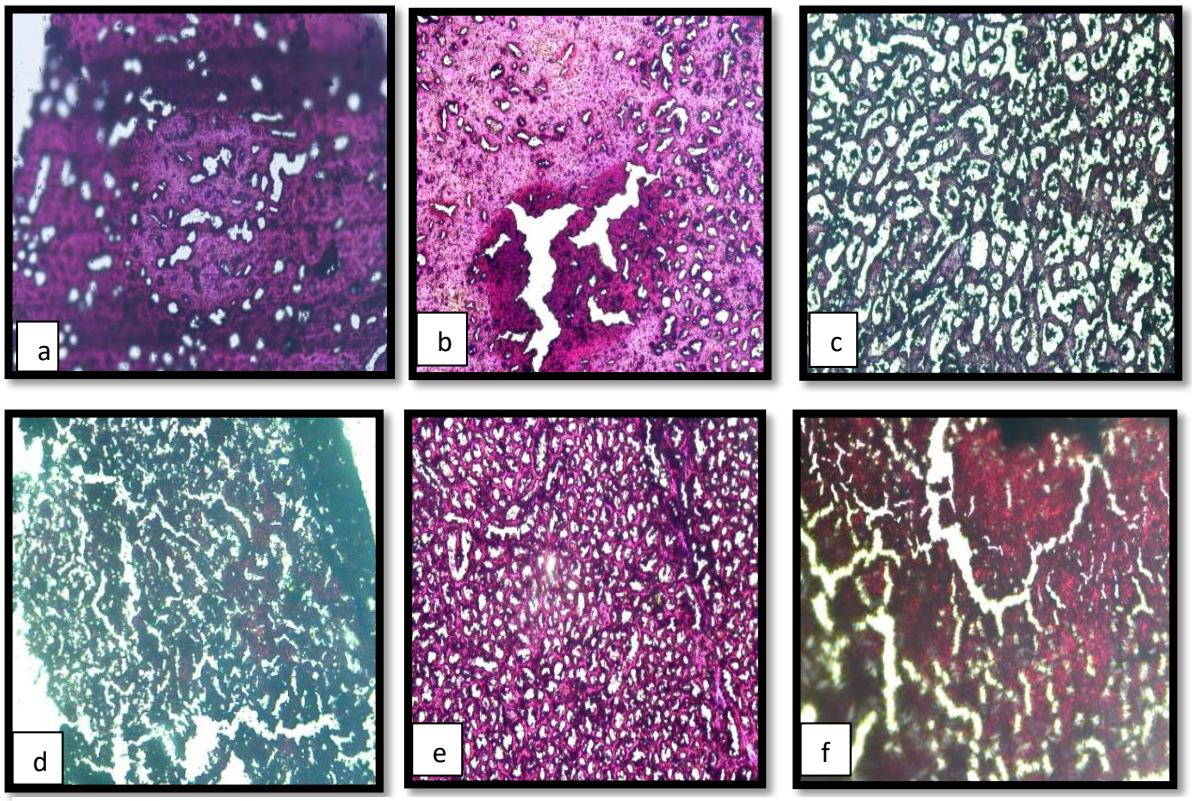

Figure 4.9.3 Histological analysis of Kidney tissues on exposure to Various Nanoparticles

a) control, (b) HcNPs (c) AjNPs, (d) VNPs (e)ZnNPs (f) Conjugate

In Vivo safety assessment of biosynthesized nanoparticles.

4.10 Effect of nanoparticles on MRSA Burden Reduction

Effect of nanoparticles on the reduction of burn wound infection was seen by generating infection model of MRSA and PA.

Mice (Balb/c) were divided into 4 groups. Mice treated with AjNPs hydrogels, mice treated with HcNPs hydrogels, mice treated with hydrogels without nanoparticles and an infection control group. The CFUs were calculated at day 1, 3, 7, 11, and 15 of treatment to analyse the antibacterial effects of these nanoparticles in vivo. CFU count of $2x10^5$ was required to establish the infection, which was seen to be maintained in the control group throughout the experiments. For hydrogel control group which devoid nanoparticles in them, they showed initial reduction near to this cut off value for infection establishment. At day 15 of experiment hydrogels were able to eliminate the infection of MRSA exhibiting their ability to reduce infection on a prolonged treatment. In the case of AjNPs the reduction to $3x10^4$ was shown at the day 3 of the infection which was the case with HcNPs as well i.e. the CFUs were reduced to $4.35x10^3$. In order to confirm the reduction is because of nanoparticle treatment and not because of the mice immune response to fight of infection nanoparticles were not treated for days 5 and 6, and the samples were taken on day 7 for CFUs measurement. It can be seen the infection was re-established when treatment was stopped. From day 7 treatment was started again to reconfirm the effect of treatment and its comparison with the control group. The effects as evident from the graph was the confirmation of the antibacterial effects of nanoparticles used in the study in vivo as the reduction in the burden was seen in case of mice model infection with MRSA after their wound establishment on the day 11 and 15. The bacterial count reduction was seen to be higher in case of group treated with HcNPs

as compared to the group treated with AjNPs. This was followed by reduction in hydrogel control group as compared to the infection control group as evident from graph below.

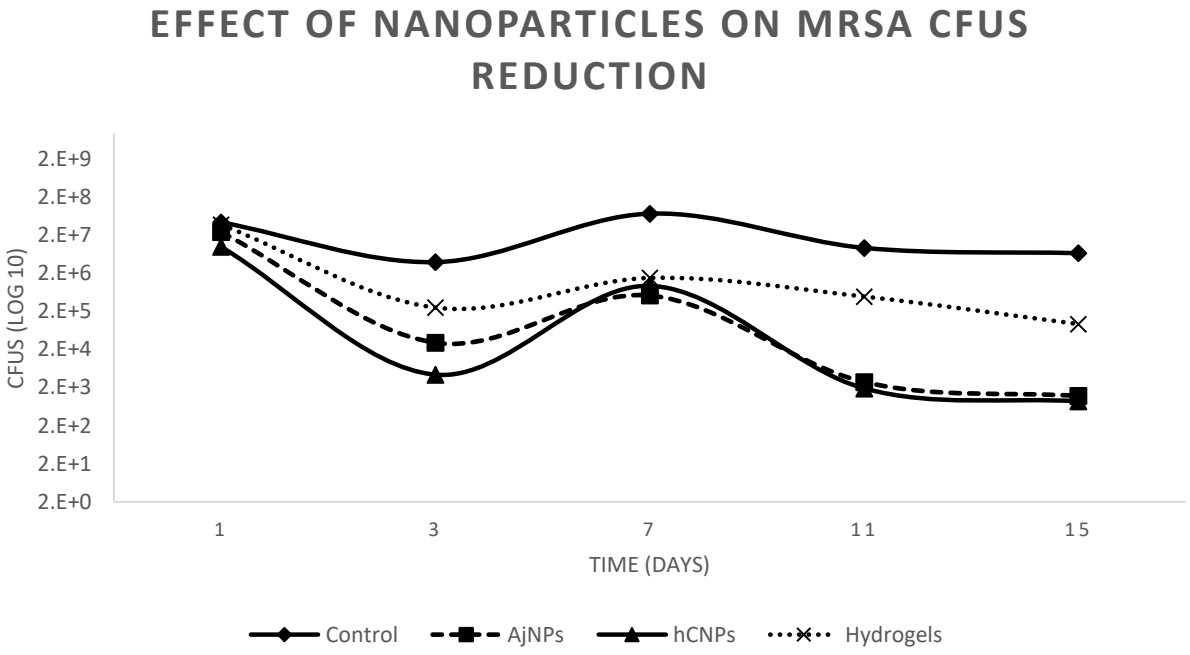

Figure 4.10.1 *Effect of nanoparticles on MRSA CFUs Reduction*

Pictures were taken to assess the recovery phase and macroscopic signs during the course of studies. These pictures showed the appearance of burn as it underwent the treatment. The 2nd degree burn infection was followed during the time course in control, hydrogel control, nanoparticles both AjNPs and HcNPs. 2 days After 2nd degree burn, the infection was given an additional 2 days were given for the infection to establish. This was followed by the start of treatment as shown in the figure below. Eschar formation can be seen on day 3 of the treatment, on HcNPs, AjNPs and chitosan. A delay in the wound recovery can be seen in all the pictures. This

is because of the infection establishment of MRSA. On day 19 complete recovery can be seen in AjNPs group and HcNPs group whereas chitosan and control group may have infection reduction but the burn wound is not completely recovered in the control group and the chitosan group.

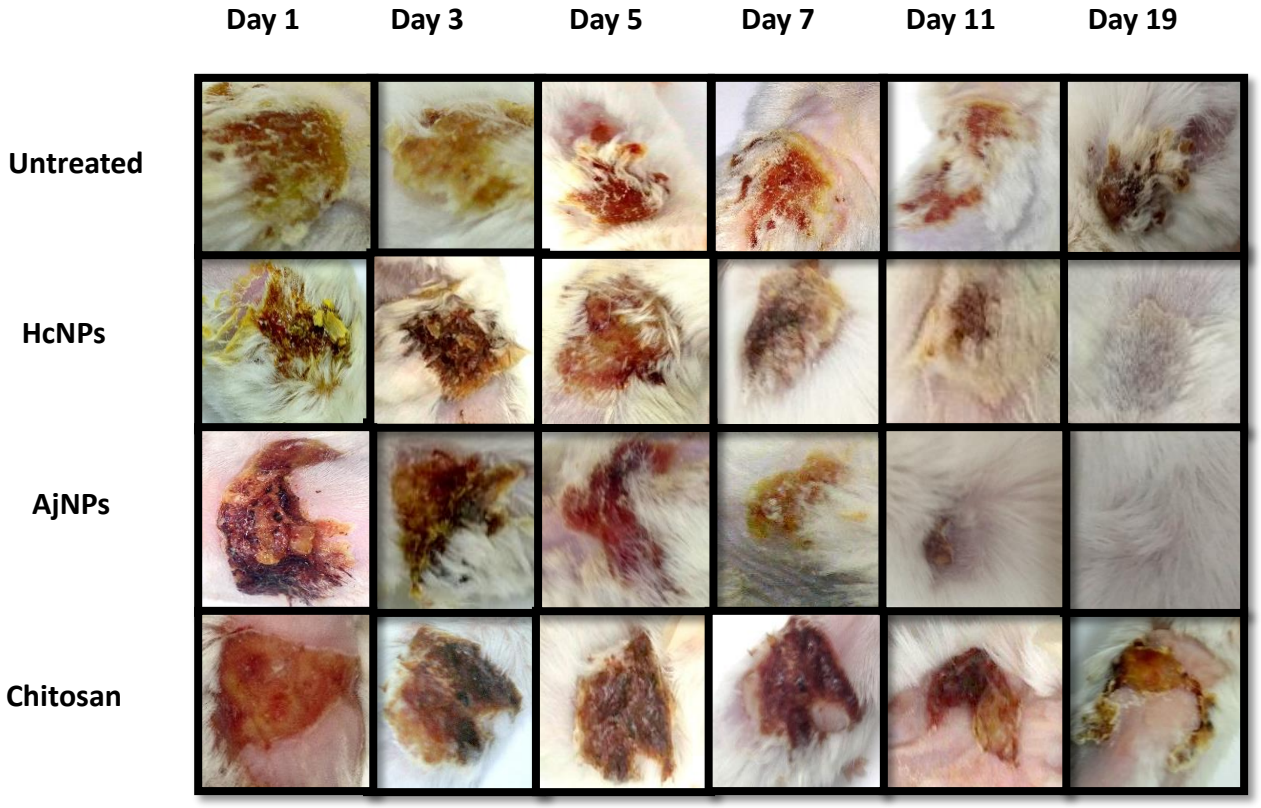

Figure 4.10.2 *Topical application on nanoparticle hydrogels against MRSA infection*

4.11 Effect of burden reduction on PA burden reduction.

Mice were divided into four groups. Mice treated with AjNPs hydrogels, mice treated with HcNPs hydrogels, mice treated with hydrogels without nanoparticles and an infection control group. The CFUs were calculated at day 1, 3, 7, 11, and 15 of treatment to analyse the antibacterial effects of these nanoparticles in vivo. CFU count of $2x10^5$ was required to establish the infection, which was seen to be maintained in the control group throughout the experiments. For hydrogel control group which devoid nanoparticles in them, they showed initial reduction near to this cut off value for infection establishment. At day 15 of experiment hydrogels were able to eliminate the infection of PA exhibiting their ability to reduce infection on a prolonged treatment. In the case of AjNPs the reduction to $2.4x10^4$ was shown at the day 3 of the infection which was the case with HcNPs as well i.e. the CFUs were reduced to $4.9x10^5$. In order to confirm the reduction is because of nanoparticle treatment and not because of the mice immune response to fight of infection nanoparticles were not treated for days 5 and 6, and the samples were taken on day 7 for CFUs measurement. It can be seen the infection was re-established when treatment was stopped. From day 7 treatment was started again to reconfirm the effect of treatment and its comparison with the control group. The effects as evident from the graph was the confirmation of the antibacterial effects of nanoparticles used in the study in vivo as the reduction in the burden was seen in case of mice model infection with PA after their wound establishment on the day 11 and 15. The bacterial count reduction was seen to be higher in case of group treated with HcNPs as compared to the group treated with AjNPs. This was followed by reduction in hydrogel control group as compared to the infection control group as evident from the graph below.

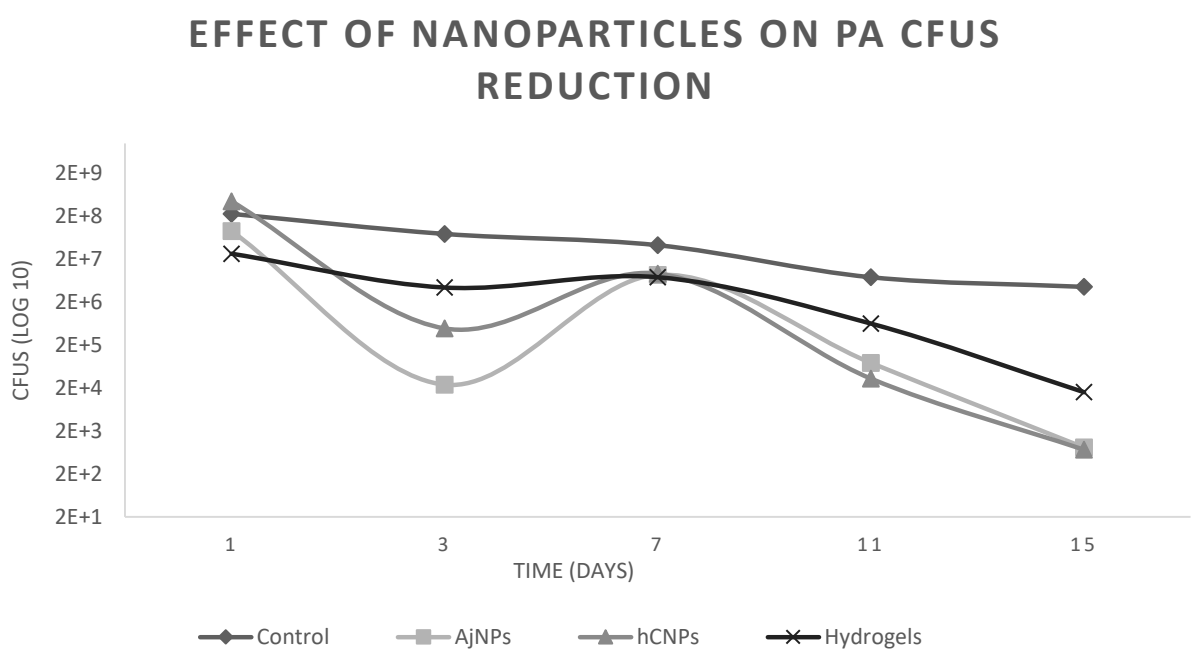

Figure 4.11.1 *Effect of nanoparticles on PA CFUs reduction*

Pictures were taken to assess the recovery phase and macroscopic signs during the course of studies. These pictures showed the appearance of burn as it underwent the treatment. The 2nd degree burn infection was followed during the time course in control, hydrogel control, nanoparticles both AjNPs and HcNPs. 2 days After 2nd degree burn, the infection was given an additional 2 days were given for the infection to establish. This was followed by the start of treatment as shown in the figure below. Eschar formation can be seen on day 5 of the treatment, on HcNPs, AjNPs and chitosan. A delay in the wound recovery can be seen in all the pictures. This is because of the infection establishment of PA. On day 19 complete recovery can be seen in AjNPs group and HcNPs group whereas chitosan and control group may have infection reduction but the burn wound is not completely recovered in the control group and the chitosan group. The results are summarized in the picture below.

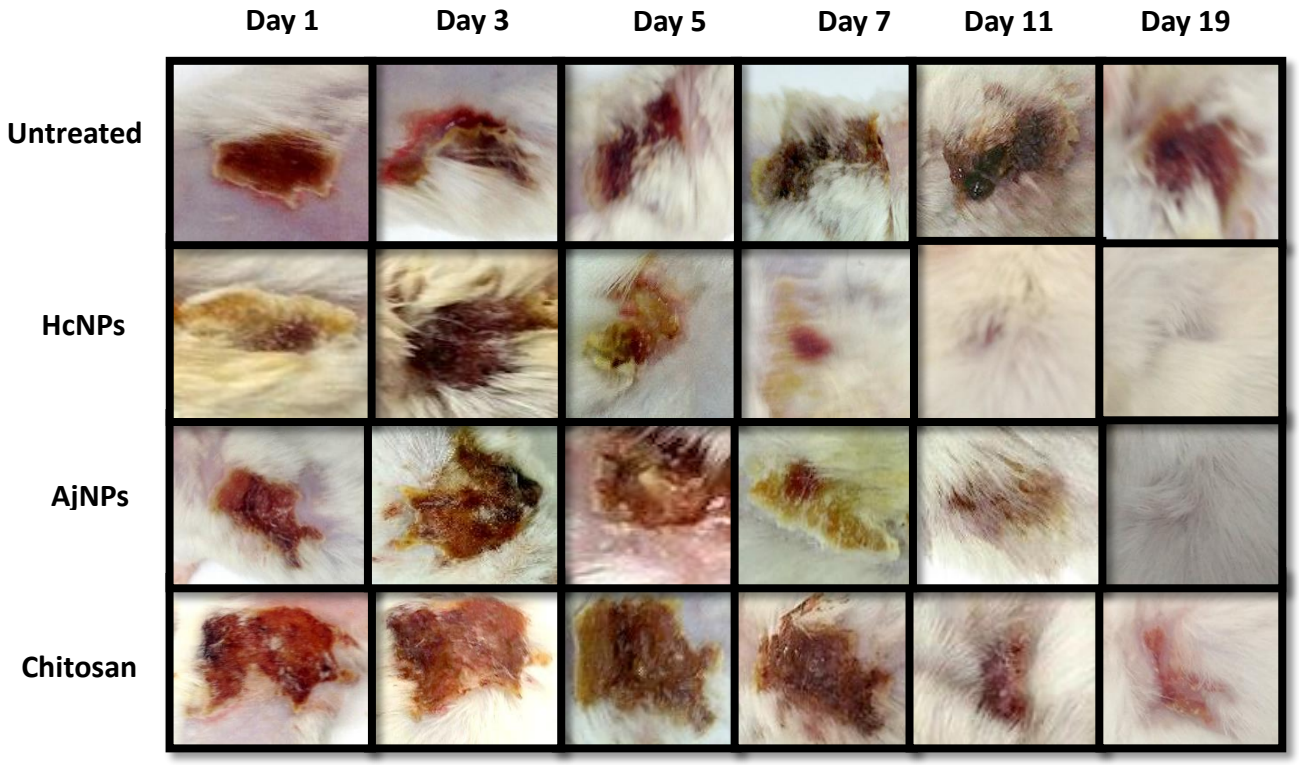

Figure 4.11.2 *Topical application on nanoparticle hydrogels against PA infection*

Chapter 5

5 Discussion

The current study was carried out to compare the in vivo efficacy of nanoparticles whose antibacterial properties have already been established. It is a well-established fact that antioxidant potential of AjNPs have been contributed to its capping agents (J. Huang et al., 2007). High antioxidant activity of AjNPs, HcNPs, and ZnNPs were shown owing to the capping agents as these nanoparticles have been synthesised using plant extract rich in flavonoids (Abdel-Aziz et al.). Plants like Aerva javanica and Heliotropium crispum are enriched source of antioxidants and using these antioxidant compounds (Phenols) in synthesis of silver nanoparticles have given us silver nanoparticles with antioxidant properties. Presence of phenols as the capping agent have already been established in the previous studies (Khan et al., 2016). Starch capped nanoparticles used in the study did not show the radical scavenging properties as compared to the AjNPs, HcNPs, ZnNPs and VNPs. CNPs were synthesised previously through the chemical route of synthesis (Arif et al 2015) as compared to the rest of nanoparticles synthesised from biological route of synthesis. Phenolic compounds present in AjNPs, HcNPs, and ZnNPs were the reason of scavenging free radicals when H_2O_2 radical scavenging assay was performed. (J. Huang et al., 2007) and as the phenolic concentration increased with increase in the concentration of nanoparticles the increase in scavenging activity was seen. VNPs capped with a purple pigment Violacein has known anticancer, antimicrobial and anticancer properties (Konzen et al., 2006). The anticancer and antibacterial studies of VNPs have been studied previously by sania arif (Unpublished results). This study was conducted to assess the radical scavenging potential and to assess their in vivo toxicity for their potential use as a drug delivery vehicle and antimicrobial agent. On comparison with AjNPs, and HcNPs, VNPs showed higher antioxidant properties at the lose dose as compared

to the high dose. This was because of the possible the scavenging potential of peroxides and superoxide of violacein (Konzen et al., 2006). Biological synthesis of nanoparticles have advantage over chemical or physical methods owing to presence of natural surface functionalizing molecules that renders nanoparticles nontoxic.

Cytotoxicity of nanoparticles increases with decrease in size which is due to increase in their surface area. Small sized nanoparticles can easily evade phagocytosis and hence excretion or degradation by cellular mechanisms. Surface capping can significantly reduce the cytotoxicity of nanoparticles. It is imperative to consider the size of nanoparticles for biomedical applications as *in-vivo* studies have confirmed that nanoparticles greater than 80 nm gets entrapped in liver and exhibit long term cytotoxicity, whereas small sized nanoparticles less than 10 nm are excreted through urine. (Gurunathan, Han, Eppakayala, Jeyaraj, & Kim, 2013). Size dependent endocytosis of nanoparticles play an important role in drug delivery as they can help drug to gain entry into the cells. Clathrin, caveolin, and dynamin mediated endocytosis have been reported along with macropinocytosis have been reported to be possible mechanisms where dynamin and clatherin mediated endocytosis occur in case of bigger particles size, particles with small size are endocytosed through caveolin (Iversen, Skotland, & Sandvig, 2011). Particles with size less than 10 nm can be efficiently diffused into the cells and hence into nucleus where they can cause increased toxicity and genotoxicity so they should be capped by nontoxic molecules to prevent their toxicity on cells (L. W. Zhang & Monteiro-Riviere, 2009)

MTT assay was performed to assess the mitochondrial damage by these nanoparticles. Nanoparticles used in the studies ranged from 20nm (ZnNPs) to 30nm (VNPs) and HcNPs (42 nm), CNPs (50nm), AjNPs (62nm). AjNPs showed no effects of mitochondrial damage on Human Colonic epithelial cell lines which are primary cell lines based on their antioxidant potential. The

absence of cytotoxicity was because of the established antioxidant capping and the size of nanoparticles. It has been shown that the nanoparticles with smaller size released more ions in the medium as compared to particles with large size. (Gliga, Skoglund, Odnevall Wallinder, Fadeel, & Karlsson, 2014). Nanoparticles with range less than 100 nm have the ability to penetrate well in the tumors. Especially nanoparticles with diameter <50nm in particular have high permeability rate. (Blanco, Shen, & Ferrari, 2015). AjNPs did not induce cytotoxicity in Huh7 and MCF7 cell lines owing to their larger size and slow or no release of silver ions in the medium (Gliga et al., 2014) and strong surface capping (Sharma et al., 2009) This may also be related to the bio distribution of AjNPs in living systems (Chernyak et al., 2006). Cytotoxicity is one major limitation in their application originating due to perturbations of physiological mechanisms by nanoparticles. Their cytotoxicity is because of three major factors size, surface to volume area and surface capping (Nair et al., 2009) . Cytotoxicity of nanoparticles increases with decrease in size which is due to increase in their surface area. Small sized nanoparticles can easily evade phagocytosis and hence excretion or degradation by cellular mechanisms. Surface capping can significantly reduce the cytotoxicity of nanoparticles. (T. Zhang, Wang, Chen, & Chen, 2014). Similar results of their nontoxicity have also been reported for HcNPs, ZnNPs, VNPs and HcNPs (Khan et al., 2016). AjNPs showed low toxicity in Huh7 cells because of negatively charged surface as it has been established that negative charged particles shows reduced toxicity due to reduction in the serum protein adsorption as compared to positively charged nanoparticles shown in various studies (Blanco et al., 2015). This also results in longer circulation half-lives as compared to positively charged particles. Positively charged nanoparticles have more non-specific cellular uptake on comparison with negatively charged nanoparticles. Cationic nanoparticles however show an edge over anionic nanoparticle in case of their delivery to tumors. It is highly

desirable for nanoparticles to be zwitter ionic in design which can switch the surface charged based on environmental pH or Stimulus.

The effect seen in IP administration of Nanoparticles during in vivo toxicity assessment co related with the size dependent properties of nanoparticles. HcNPs being <50 nm in diameter showed minute accumulation in Liver and spleen upon treatment as compared to VNPs and Conjugate. The increase in accumulation was because of their small size and possible aggregation in the medium. VNPs showed inflammation possibly because of ion release mechanism from the core as established earlier being smaller in size than AjNPs (Gliga et al., 2014).

Weight loss as evident from the nanoparticle study was seen much more in VNPs as compared to rest of nanoparticles used in the study. This reduction in the weight is attributed to their accumulation in liver and spleen as seen in the histological analysis causing inflammation in ducts. It is also postulated that Violacein capped silver nanoparticles might have interacted with the glycocalyx of intestine after gaining entry into circulatory system and bringing about structural changes that would have changed the microvillus permeability and hence resulted in microvilli damage .and hence reduction in body weight (Shahare & Yashpal, 2013). This effect would have been much more evident if nanoparticles were administered orally instead of intraperitoneal administration. Owing to size and surface charge of VNPs, they were recognized by Kupffer cells of the liver and accumulation was hence seen in liver causing hepatomegaly along with hepatocyte generation as explained in results.

Results shown by efficacy assessment of biosynthesid nanoparticles in vivo were synchronous to the results obtained in vitro against MRSA and PA during the assessment of antimicrobial studies.

Chitosan hydrogels used in the current studies were used owing to the low toxicity and biodegradability (Veiga & Schneider, 2013) . Nanoparticle incorporated in the hydrogels showed immediate effects and burden reduction in both MRSA and PA cases because of their release on contact with the infected wounds (Gordon, Saupe, McBurney, Rades, & Hook, 2008). The burden reduction showed the possible mechanism of disrupting the biofilm as evident from the antibiofilm activity of HcNPs (Khan et al., 2016).

These results effectively exhibit the role of AjNPs and HcNPs as disinfectants and to be use ad drug delivery vehicle owing to their safety profile, antioxidant properties and excellent antimicrobial properties obtained in this study. Nanoparticles which are biosynthesize have alkylating agents (Schrand, Dai, Schlager, & Hussain, 2012) like phenols used often to lower cytotoxicity and this was the reason these biosynthesized nanoparticles were not cytotoxic to cells because of their innate antioxidant potential and at the same time had antimicrobial properties which proved to be right during in vivo studies.

Conclusion

Five nanoparticles that had already been synthesized in previous studies were compared during this study and screened out owing to their properties. They were first undergone through the antioxidant potential and starch capped nanoparticles (CNPs) on the basis of very low antioxidant potential even at the higher doses were eliminated. Rest of the nanoparticles used in the studied were screened through in vitro toxicity assessment and all the four nanoparticles passed out this stage of analysis. This resulted in the comparison on in vitro antimicrobial properties against in vivo and ZnNPs were expelled owing to their very high MIC of 20 mg/ml. the remaining three nanoparticles AjNPs, HcNPs, and VNPs were then analyzed for their safety in terms of morbidity and mortality rates along with toxicity in liver, spleen and kidney. VNPs showing hepatomegaly, splenomegaly, and high weight reduction, tissue damage to great extent and because of their high mortality were excluded and AjNPs and HcNPs were evaluated finally for their in vivo potential for burn wound infections against which they were found efficacious. Hence out of five nanoparticles two nanoparticles with best antimicrobial properties along with excellent safety profiles were screened out and these were silver nanoparticles synthesized from *Aerva javanica* (AjNPs) and *Heliotropium crispum* (HcNPs).

Future Prospects

These nanoparticles can be used in the filter membranes that would be used in the water purification and filter assembly. Furthermore these nanoparticles can be used to coat surgical instruments including surgical blades and sutures using dip coating, electrodeposition, or layer by layer coating. These can be used in fabrics that can be used in hospital settings to prevent the spread of nosocomial infections. Nanoparticles will be used in drug delivery for treatment of cancer e.g it can be conjugated with faslodex to treat breast cancer. Further characterization of these nanoparticles to study its effects in SOD, GSH gene regulation will give an insight into its mechanism in checking ROS generation and its effect on regulation of p53, and other pro-apoptotic genes would strengthen its application on a broader range.

Chapter 6

References

Abdel-Aziz, M. S., Shaheen, M. S., El-Nekeety, A. A., & Abdel-Wahhab, M. A. Antioxidant and antibacterial activity of silver nanoparticles biosynthesized using Chenopodium murale leaf extract. (0).

Aloush, V., Navon-Venezia, S., Seigman-Igra, Y., Cabili, S., & Carmeli, Y. (2006). Multidrug-resistant Pseudomonas aeruginosa: risk factors and clinical impact. *Antimicrobial agents and chemotherapy, 50*(1), 43-48.

Anderson, M. F., Nilsson, M., Eriksson, P. S., & Sims, N. R. (2004). Glutathione monoethyl ester provides neuroprotection in a rat model of stroke. *Neurosci Lett, 354*(2), 163-165.

Arias, J. L., Gallardo, V., Gomez-Lopera, S. A., Plaza, R. C., & Delgado, A. V. (2001). Synthesis and characterization of poly(ethyl-2-cyanoacrylate) nanoparticles with a magnetic core. *J Control Release, 77*(3), 309-321.

Arora, S., Jain, J., Rajwade, J. M., & Paknikar, K. M. (2008). Cellular responses induced by silver nanoparticles: In vitro studies. *Toxicol Lett, 179*(2), 93-100. doi:10.1016/j.toxlet.2008.04.009

Beevi, S. S., Narasu, M. L., & Gowda, B. B. (2010). Polyphenolics profile, antioxidant and radical scavenging activity of leaves and stem of Raphanus sativus L. *Plant Foods Hum Nutr, 65*(1), 8-17. doi:10.1007/s11130-009-0148-6

Behra, R., Sigg, L., Clift, M. J., Herzog, F., Minghetti, M., Johnston, B., . . . Rothen-Rutishauser, B. (2013). Bioavailability of silver nanoparticles and ions: from a chemical and biochemical perspective. *Journal of The Royal Society Interface, 10*(87), 20130396.

Blanco, E., Shen, H., & Ferrari, M. (2015). Principles of nanoparticle design for overcoming biological barriers to drug delivery. *Nat Biotech, 33*(9), 941-951. doi:10.1038/nbt.3330

Bueno, V. B., Bentini, R., Catalani, L. H., & Petri, D. F. S. (2013). Synthesis and swelling behavior of xanthan-based hydrogels. *Carbohydrate Polymers, 92*(2), 1091-1099. doi:http://dx.doi.org/10.1016/j.carbpol.2012.10.062

Chaloupka, K., Malam, Y., & Seifalian, A. M. (2010). Nanosilver as a new generation of nanoproduct in biomedical applications. *Trends in Biotechnology, 28*(11), 580-588. doi:http://dx.doi.org/10.1016/j.tibtech.2010.07.006

Cheeseman, K. H., & Slater, T. F. (1993). An introduction to free radical biochemistry. *Br Med Bull, 49*(3), 481-493.

Cheppudira, B., Fowler, M., McGhee, L., Greer, A., Mares, A., Petz, L., . . . Clifford, J. L. (2013). Curcumin: a novel therapeutic for burn pain and wound healing. *Expert Opin Investig Drugs, 22*(10), 1295-1303. doi:10.1517/13543784.2013.825249

Chernyak, B. V., Izyumov, D. S., Lyamzaev, K. G., Pashkovskaya, A. A., Pletjushkina, O. Y., Antonenko, Y. N., . . . Skulachev, V. P. (2006). Production of reactive oxygen species in mitochondria of HeLa cells under oxidative stress. *Biochimica et Biophysica Acta (BBA) - Bioenergetics, 1757*(5–6), 525-534. doi:http://dx.doi.org/10.1016/j.bbabio.2006.02.019

Clarke, J., Wu, H. C., Jayasinghe, L., Patel, A., Reid, S., & Bayley, H. (2009). Continuous base identification for single-molecule nanopore DNA sequencing. *Nat Nanotechnol, 4*(4), 265-270. doi:10.1038/nnano.2009.12

Costerton, W., Veeh, R., Shirtliff, M., Pasmore, M., Post, C., & Ehrlich, G. (2003). The application of biofilm science to the study and control of chronic bacterial infections. *The Journal of clinical investigation, 112*(10), 1466-1477.

Curnutte, J. T. (2004). Superoxide production by phagocytic leukocytes: the scientific legacy of Bernard Babior. *Journal of Clinical Investigation, 114*(8), 1054-1057. doi:10.1172/JCI200423377

Danese, P. N. (2002). Antibiofilm approaches: prevention of catheter colonization. *Chemistry & biology, 9*(8), 873-880.

Dar, M. A., Ingle, A., & Rai, M. (2013). Enhanced antimicrobial activity of silver nanoparticles synthesized by Cryphonectria sp. evaluated singly and in combination with antibiotics. *Nanomedicine: Nanotechnology, Biology and Medicine, 9*(1), 105-110. doi:http://dx.doi.org/10.1016/j.nano.2012.04.007

Davis, S. C., Ricotti, C., Cazzaniga, A., Welsh, E., Eaglstein, W. H., & Mertz, P. M. (2008). Microscopic and physiologic evidence for biofilm-associated wound colonization in vivo. *Wound Repair Regen, 16*(1), 23-29. doi:10.1111/j.1524-475X.2007.00303.x

Dewanjee, S., Maiti, A., Sahu, R., Dua, T. K., & Mandal, V. (2011). Effective Control of Type 2 Diabetes through Antioxidant Defense by Edible Fruits of Diospyros peregrina. *Evid Based Complement Alternat Med, 2011*, 675397. doi:10.1093/ecam/nep080

Dijkshoorn, L., Nemec, A., & Seifert, H. (2007). An increasing threat in hospitals: multidrug-resistant Acinetobacter baumannii. *Nature Reviews Microbiology, 5*(12), 939-951.

Edwards, R., & Harding, K. G. (2004). Bacteria and wound healing. *Curr Opin Infect Dis, 17*(2), 91-96.

Eijsink, V., Hoell, I., & Vaaje-Kolstada, G. (2010). Structure and function of enzymes acting on chitin and chitosan. *Biotechnol Genet Eng Rev, 27*, 331-366.

Emerich, D. F., & Thanos, C. G. (2006). The pinpoint promise of nanoparticle-based drug delivery and molecular diagnosis. *Biomolecular Engineering, 23*(4), 171-184. doi:http://dx.doi.org/10.1016/j.bioeng.2006.05.026

Emori, T. G., & Gaynes, R. P. (1993). An overview of nosocomial infections, including the role of the microbiology laboratory. *Clinical microbiology reviews, 6*(4), 428-442.

Feng, Q., Wu, J., Chen, G., Cui, F., Kim, T., & Kim, J. (2000). A mechanistic study of the antibacterial effect of silver ions on Escherichia coli and Staphylococcus aureus. *Journal of biomedical materials research, 52*(4), 662-668.

Gliga, A. R., Skoglund, S., Odnevall Wallinder, I., Fadeel, B., & Karlsson, H. L. (2014). Size-dependent cytotoxicity of silver nanoparticles in human lung cells: the role of cellular uptake, agglomeration and Ag release. *Particle and Fibre Toxicology, 11*(1), 11. doi:10.1186/1743-8977-11-11

Goddard Iii, W. A., Brenner, D., Lyshevski, S. E., & Iafrate, G. J. (2007). *Handbook of nanoscience, engineering, and technology*: CRC press.

Gordon, S., Saupe, A., McBurney, W., Rades, T., & Hook, S. (2008). Comparison of chitosan nanoparticles and chitosan hydrogels for vaccine delivery. *J Pharm Pharmacol, 60*(12), 1591-1600. doi:10.1211/jpp/60.12.0004

Gurunathan, S., Han, J. W., Eppakayala, V., Jeyaraj, M., & Kim, J. H. (2013). Cytotoxicity of biologically synthesized silver nanoparticles in MDA-MB-231 human breast cancer cells. *Biomed Res Int, 2013*, 535796. doi:10.1155/2013/535796

Horvath, E. E., Murray, C. K., Vaughan, G. M., Chung, K. K., Hospenthal, D. R., Wade, C. E., . . . Cancio, L. C. (2007). Fungal wound infection (not colonization) is independently

associated with mortality in burn patients. *Ann Surg, 245*(6), 978-985. doi:10.1097/01.sla.0000256914.16754.80

Hsin, Y. H., Chen, C. F., Huang, S., Shih, T. S., Lai, P. S., & Chueh, P. J. (2008). The apoptotic effect of nanosilver is mediated by a ROS- and JNK-dependent mechanism involving the mitochondrial pathway in NIH3T3 cells. *Toxicol Lett, 179*(3), 130-139. doi:10.1016/j.toxlet.2008.04.015

Huang, J., Li, Q., Sun, D., Lu, Y., Su, Y., Yang, X., . . . He, N. (2007). Biosynthesis of silver and gold nanoparticles by novel sundried Cinnamomum camphora leaf. *Nanotechnology, 18*(10), 105104.

Huang, L., Dai, T., Xuan, Y., Tegos, G. P., & Hamblin, M. R. (2011). Synergistic combination of chitosan acetate with nanoparticle silver as a topical antimicrobial: efficacy against bacterial burn infections. *Antimicrobial agents and chemotherapy, 55*(7), 3432-3438.

Ignarro, L. J. (1990). Nitric oxide. A novel signal transduction mechanism for transcellular communication. *Hypertension, 16*(5), 477-483.

Iversen, T.-G., Skotland, T., & Sandvig, K. (2011). Endocytosis and intracellular transport of nanoparticles: Present knowledge and need for future studies. *Nano Today, 6*(2), 176-185. doi:http://dx.doi.org/10.1016/j.nantod.2011.02.003

Jain, J., Arora, S., Rajwade, J. M., Omray, P., Khandelwal, S., & Paknikar, K. M. (2009). Silver nanoparticles in therapeutics: development of an antimicrobial gel formulation for topical use. *Molecular Pharmaceutics, 6*(5), 1388-1401.

Kalishwaralal, K., BarathManiKanth, S., Pandian, S. R. K., Deepak, V., & Gurunathan, S. (2010). Silver nanoparticles impede the biofilm formation by< i> Pseudomonas aeruginosa</i>

and< i> Staphylococcus epidermidis</i>. *Colloids and Surfaces B: Biointerfaces, 79*(2), 340-344.

Kassaee, M. Z., Mohammadkhani, M., Akhavan, A., & Mohammadi, R. (2011). In situ formation of silver nanoparticles in PMMA via reduction of silver ions by butylated hydroxytoluene. *Structural Chemistry*, *22*(1), 11-15. doi:10.1007/s11224-010-9671-1

Khan, F., Hashmi, M. U., Khalid, N., Hayat, M. Q., Ikram, A., & Janjua, H. A. (2016). Controlled assembly of silver nano-fluid in Heliotropium crispum extract: A potent anti-biofilm and bactericidal formulation. *Applied Surface Science, 387*, 317-331. doi:http://dx.doi.org/10.1016/j.apsusc.2016.05.133

Kim, J. S., Kuk, E., Yu, K. N., Kim, J.-H., Park, S. J., Lee, H. J., . . . Hwang, C.-Y. (2007). Antimicrobial effects of silver nanoparticles. *Nanomedicine: Nanotechnology, Biology and Medicine, 3*(1), 95-101.

Kim, J. S., Kuk, E., Yu, K. N., Kim, J. H., Park, S. J., Lee, H. J., . . . Cho, M. H. (2007). Antimicrobial effects of silver nanoparticles. *Nanomedicine, 3*(1), 95-101. doi:10.1016/j.nano.2006.12.001

Kim, S., Choi, J. E., Choi, J., Chung, K. H., Park, K., Yi, J., & Ryu, D. Y. (2009). Oxidative stress-dependent toxicity of silver nanoparticles in human hepatoma cells. *Toxicol In Vitro, 23*(6), 1076-1084. doi:10.1016/j.tiv.2009.06.001

Kittler, S., Greulich, C., Diendorf, J., Koller, M., & Epple, M. (2010). Toxicity of silver nanoparticles increases during storage because of slow dissolution under release of silver ions. *Chem Mat, 22*. doi:10.1021/cm100023p

Klueh, U., Wagner, V., Kelly, S., Johnson, A., & Bryers, J. D. (2000). Efficacy of silver-coated fabric to prevent bacterial colonization and subsequent device-based biofilm formation. *Journal of biomedical materials research, 53*(6), 621-631.

Konorev, E. A., Hogg, N., & Kalyanaraman, B. (1998). Rapid and irreversible inhibition of creatine kinase by peroxynitrite. *FEBS Lett, 427*(2), 171-174.

Konzen, M., De Marco, D., Cordova, C. A. S., Vieira, T. O., Antônio, R. V., & Creczynski-Pasa, T. B. (2006). Antioxidant properties of violacein: Possible relation on its biological function. *Bioorganic & Medicinal Chemistry, 14*(24), 8307-8313. doi:http://dx.doi.org/10.1016/j.bmc.2006.09.013

Levy, S. B., & Marshall, B. (2004). Antibacterial resistance worldwide: causes, challenges and responses. *Nature medicine, 10*, S122-S129.

Li, X., Xu, H., Chen, Z.-S., & Chen, G. (2011). Biosynthesis of Nanoparticles by Microorganisms and Their Applications. *Journal of Nanomaterials, 2011*, 16. doi:10.1155/2011/270974

Liu, M., & Guyot-Sionnest, P. (2004). Synthesis and optical characterization of Au/Ag core/shell nanorods. *The Journal of Physical Chemistry B, 108*(19), 5882-5888.

Liu, S., Ng, A. K., Xu, R., Wei, J., Tan, C. M., Yang, Y., & Chen, Y. (2010). Antibacterial action of dispersed single-walled carbon nanotubes on Escherichia coli and Bacillus subtilis investigated by atomic force microscopy. *Nanoscale, 2*(12), 2744-2750. doi:10.1039/c0nr00441c

Lovric, J., Bazzi, H. S., Cuie, Y., Fortin, G. R., Winnik, F. M., & Maysinger, D. (2005). Differences in subcellular distribution and toxicity of green and red emitting CdTe quantum dots. *J Mol Med (Berl), 83*(5), 377-385. doi:10.1007/s00109-004-0629-x

Maneerung, T., Tokura, S., & Rujiravanit, R. (2008). Impregnation of silver nanoparticles into bacterial cellulose for antimicrobial wound dressing. *Carbohydrate polymers, 72*(1), 43-51.

Martindale, J. L., & Holbrook, N. J. (2002). Cellular response to oxidative stress: signaling for suicide and survival. *J Cell Physiol, 192*(1), 1-15. doi:10.1002/jcp.10119

Martínez-Castañón, G. A., Niño-Martínez, N., Martínez-Gutierrez, F., Martínez-Mendoza, J. R., & Ruiz, F. (2008). Synthesis and antibacterial activity of silver nanoparticles with different sizes. *Journal of Nanoparticle Research, 10*(8), 1343-1348.

Matsumura, Y., Yoshikata, K., Kunisaki, S.-i., & Tsuchido, T. (2003). Mode of bactericidal action of silver zeolite and its comparison with that of silver nitrate. *Applied and environmental microbiology, 69*(7), 4278-4281.

Maynard, S., Schurman, S. H., Harboe, C., de Souza-Pinto, N. C., & Bohr, V. A. (2009). Base excision repair of oxidative DNA damage and association with cancer and aging. *Carcinogenesis, 30*(1), 2-10.

McGowan, J. E. (1983). Antimicrobial Resistance in Hospital Organisms and Its Relation to Antibiotic Use. *Review of Infectious Diseases, 5*(6), 1033-1048. doi:10.1093/clinids/5.6.1033

Medintz, I. L., Uyeda, H. T., Goldman, E. R., & Mattoussi, H. (2005). Quantum dot bioconjugates for imaging, labelling and sensing. *Nat Mater, 4*(6), 435-446. doi:10.1038/nmat1390

Menke, N. B., Ward, K. R., Witten, T. M., Bonchev, D. G., & Diegelmann, R. F. (2007). Impaired wound healing. *Clin Dermatol, 25*(1), 19-25. doi:10.1016/j.clindermatol.2006.12.005

Morones, J. R., Elechiguerra, J. L., Camacho, A., Holt, K., Kouri, J. B., Ramírez, J. T., & Yacaman, M. J. (2005). The bactericidal effect of silver nanoparticles. *Nanotechnology, 16*(10), 2346.

Nair, S., Sasidharan, A., Divya Rani, V. V., Menon, D., Nair, S., Manzoor, K., & Raina, S. (2009). Role of size scale of ZnO nanoparticles and microparticles on toxicity toward bacteria and osteoblast cancer cells. *Journal of Materials Science: Materials in Medicine, 20*(1), 235-241. doi:10.1007/s10856-008-3548-5

- Nanofibrous Structure of Chitosan for Biomedical Applications. - *Journal of Nanomedicine & Biotherapeutic Discovery*(- 1), -. doi:- 10.4172/2155-983x.1000102

Perelshtein, I., Applerot, G., Perkas, N., Wehrschetz-Sigl, E., Hasmann, A., Guebitz, G. M., & Gedanken, A. (2008). Antibacterial Properties of an In Situ Generated and Simultaneously Deposited Nanocrystalline ZnO on Fabrics. *ACS Applied Materials & Interfaces, 1*(2), 361-366. doi:10.1021/am8000743

Pietta, P. G. (2000). Flavonoids as antioxidants. *J Nat Prod, 63*(7), 1035-1042.

Rai, M., Yadav, A., & Gade, A. (2009). Silver nanoparticles as a new generation of antimicrobials. *Biotechnology Advances, 27*(1), 76-83. doi:http://dx.doi.org/10.1016/j.biotechadv.2008.09.002

Rigo, C., Ferroni, L., Tocco, I., Roman, M., Munivrana, I., Gardin, C., . . . Barbante, C. (2013). Active silver nanoparticles for wound healing. *International journal of molecular sciences, 14*(3), 4817-4840.

Rujitanaroj, P.-o., Pimpha, N., & Supaphol, P. (2008). Wound-dressing materials with antibacterial activity from electrospun gelatin fiber mats containing silver nanoparticles. *Polymer, 49*(21), 4723-4732.

Salata, O. (2004). Applications of nanoparticles in biology and medicine. *J Nanobiotechnology, 2*(1), 3. doi:10.1186/1477-3155-2-3

Schaberg, D. R., Culver, D. H., & Gaynes, R. P. (1991). Major trends in the microbial etiology of nosocomial infection. *The American Journal of Medicine, 91*(3, Supplement 2), S72-S75. doi:http://dx.doi.org/10.1016/0002-9343(91)90346-Y

Schrand, A., Dai, L., Schlager, J., & Hussain, S. (2012). Toxicity Testing of Nanomaterials. In M. Balls, R. Combes, & N. Bhogal (Eds.), *New Technologies for Toxicity Testing* (Vol. 745, pp. 58-75): Springer US.

Shahare, B., & Yashpal, M. (2013). Toxic effects of repeated oral exposure of silver nanoparticles on small intestine mucosa of mice. *Toxicol Mech Methods, 23*(3), 161-167. doi:10.3109/15376516.2013.764950

Sharma, V. K., Yngard, R. A., & Lin, Y. (2009). Silver nanoparticles: green synthesis and their antimicrobial activities. *Adv Colloid Interface Sci, 145*(1-2), 83-96. doi:10.1016/j.cis.2008.09.002

Shim, J., Seok Kang, H., Park, W. S., Han, S. H., Kim, J., & Chang, I. S. (2004). Transdermal delivery of mixnoxidil with block copolymer nanoparticles. *J Control Release, 97*(3), 477-484. doi:10.1016/j.jconrel.2004.03.028

Silva, G. A. (2004). Introduction to nanotechnology and its applications to medicine. *Surgical Neurology, 61*(3), 216-220. doi:http://dx.doi.org/10.1016/j.surneu.2003.09.036

Slaughter, B. V., Khurshid, S. S., Fisher, O. Z., Khademhosseini, A., & Peppas, N. A. (2009). Hydrogels in regenerative medicine. *Adv Mater, 21*(32-33), 3307-3329. doi:10.1002/adma.200802106

Taraszkiewicz, A., Fila, G., Grinholc, M., & Nakonieczna, J. (2012). Innovative strategies to overcome biofilm resistance. *BioMed research international, 2013*.

Thakkar, K. N., Mhatre, S. S., & Parikh, R. Y. (2010). Biological synthesis of metallic nanoparticles. *Nanomedicine: Nanotechnology, Biology and Medicine, 6*(2), 257-262. doi:http://dx.doi.org/10.1016/j.nano.2009.07.002

Tian, J., Wong, K. K. Y., Ho, C. M., Lok, C. N., Yu, W. Y., Che, C. M., . . . Tam, P. K. H. (2007). Topical delivery of silver nanoparticles promotes wound healing. *ChemMedChem, 2*(1), 129-136.

Tomaszewska, E., Soliwoda, K., Kadziola, K., Tkacz-Szczesna, B., Celichowski, G., Cichomski, M., . . . Grobelny, J. (2013). Detection limits of DLS and UV–vis spectroscopy in characterization of polydisperse nanoparticles colloids. *J Nanomaterials, 2013*. doi:10.1155/2013/313081

Trachootham, D., Zhou, Y., Zhang, H., Demizu, Y., Chen, Z., Pelicano, H., . . . Huang, P. (2006). Selective killing of oncogenically transformed cells through a ROS-mediated mechanism by beta-phenylethyl isothiocyanate. *Cancer Cell, 10*(3), 241-252. doi:10.1016/j.ccr.2006.08.009

Veiga, A. S., & Schneider, J. P. (2013). Antimicrobial hydrogels for the treatment of infection. *Biopolymers, 100*(6), 637-644. doi:10.1002/bip.22412

Verrax, J., Pedrosa, R. C., Beck, R., Dejeans, N., Taper, H., & Calderon, P. B. (2009). In situ modulation of oxidative stress: a novel and efficient strategy to kill cancer cells. *Curr Med Chem, 16*(15), 1821-1830.

Wilkinson, L. J., White, R. J., & Chipman, J. K. (2011). Silver and nanoparticles of silver in wound dressings: a review of efficacy and safety. *journal of wound care, 20*(11), 543-549.

Yamanaka, M., Hara, K., & Kudo, J. (2005). Bactericidal actions of a silver ion solution on Escherichia coli, studied by energy-filtering transmission electron microscopy and proteomic analysis. *Applied and environmental microbiology, 71*(11), 7589-7593.

Zhang, L. W., & Monteiro-Riviere, N. A. (2009). Mechanisms of quantum dot nanoparticle cellular uptake. *Toxicol Sci, 110*. doi:10.1093/toxsci/kfp087

Zhang, T., Wang, L., Chen, Q., & Chen, C. (2014). Cytotoxic Potential of Silver Nanoparticles. *Yonsei Medical Journal, 55*(2), 283-291. doi:10.3349/ymj.2014.55.2.283

Zhang, Y., Bai, Y., Jia, J., Gao, N., Li, Y., Zhang, R., . . . Yan, B. (2014). Perturbation of physiological systems by nanoparticles. *Chemical Society Reviews, 43*(10), 3762-3809.